Extraterrestrial hydroxy amino acids in CM and CR carbonaceous chondrites

Toshiki Koga[1,*], Eric T. Parker[2], Hannah L. McLain[2, 3], José C. Aponte[2, 3], Jamie E. Elsila[2], Jason P. Dworkin[2], Daniel P. Glavin[2], and Hiroshi Naraoka[1]

[1]Department of Earth and Planetary Sciences, Kyushu University, 744 Motooka, Nishi-ku, Fukuoka 819-0395, Japan

[2]NASA Goddard Space Flight Center, Greenbelt, Maryland 20771, USA

[3]Catholic University of America, Washington, District of Columbia 20064, USA

*Corresponding author: E-mail: koga.toshiki.590@s.kyushu-u.ac.jp and kogatoshiki590@gmail.com

ABSTRACT

The abundances, distributions, and enantiomeric ratios of a family of three- and four-carbon hydroxy amino acids (HAAs) were investigated in extracts of five CM and four CR carbonaceous chondrites by gas chromatography-mass spectrometry (GC-MS) analyses. Hydroxy amino acids were detected in both the acid hydrolysates of the hot water extracts and the 6 M HCl extracts of all the CM and CR chondrites analyzed here with total hot water and HCl extractable HAA concentrations ranging from 6.94 to 315 nmol per gram. The HAA analyses performed in this study revealed: 1) the combined (hot water + HCl) extracts of CR2 chondrites contained greater abundances of α-HAAs than that of CM2 chondrites and 2) the combined extracts of CM and CR chondrites contained roughly similar abundances of β- and γ-HAAs. Application of the new GC-MS method developed here resulted in the first successful chromatographic resolution of the enantiomers of an α-dialkyl HAA, D,L-α-methylserine, in carbonaceous chondrite extracts. Meteoritic α-methylserine was found to be mostly racemic within error and did not show L-enantiomeric excesses correlating with the degree of aqueous alteration, a phenomenon observed in meteoritic isovaline, another α-dialkyl amino acid. The HAAs identified in CM and CR chondrite extracts could have been produced during parent body alteration from the Strecker cyanohydrin reaction (for α-HAAs) and an ammonia-involved formose-like

reaction (for β-, and γ-HAAs).

INTRODUCTION

Amino acids are among the most intriguing soluble organic compounds found in meteorites and provide clues regarding the chemical evolution processes in the early solar system that likely set the stage for the origin of life (Chyba and Sagan 1992). The amino acid compositions of a variety of carbonaceous chondrites have been extensively examined over the past 50 years. During this period, analytical methods for amino acids have continuously improved, enabling the ability to chromatographically separate amino acid structural isomers and enantiomers, and to detect trace quantities of amino acids (*e.g.*, Glavin et al. 2018 and references therein; Simkus et al. 2019; Glavin et al. 2020a,b).

By applying increasingly improved analytical techniques to study the amino acid chemistry of meteorites, new information has been revealed to suggest that the distribution of structural isomers of meteoritic amino acids provides insight into the formation mechanisms of these aliphatic compounds and the possible processing histories of the meteorite parent bodies (Elsila et al. 2016 and references therein). For example, the relative abundances of the C_5 amino acid isomers as a function of amine position (α-, β-, γ-, or δ-) are significantly different between unaltered and aqueously altered carbonaceous chondrites (Glavin et al. 2006, 2010, 2020b; Glavin and Dworkin 2009; Burton et al. 2014). The less or moderately aqueously altered

carbonaceous chondrites (*e.g.,* CM2, CR2, and CR3) possess an amino acid distribution that is dominated by α-amino acids (Glavin et al. 2006, 2010). For example, the CM2 Murchison meteorite possesses predominantly α-amino acids, including glycine, alanine, and α-aminoisobutyric acid, which were hypothesized to have formed by the Strecker cyanohydrin synthesis, based on the coexistence of their corresponding α-hydroxy acids and α-iminodicarboxylic acids that are also products of Strecker synthesis (Peltzer and Bada 1978; Peltzer et al. 1984; Lerner and Cooper 2005). In contrast, the heavily aqueously altered chondrites (*e.g.,* CI1, CM1, and CR1) possess greater relative abundances of β-, γ-, and δ-amino acids compared to α-amino acids (Glavin et al. 2006, 2010; Elsila et al. 2016). This observation may be due to the hydrolysis of lactams and the thermal decarboxylation of α-amino dicarboxylic acids (Cooper and Cronin 1995; Glavin et al. 2010), or may correspond to differences in their degradation rates under hydrothermal conditions (Li and Brill, 2003). In either scenario, amino acid syntheses and degradations require exposure of the precursor compounds, and amino acids themselves, to liquid water (Glavin et al. 2018). Therefore, the aqueous alteration of meteorite parent bodies is thought to play a crucial role in influencing the distributions of meteoritic amino acids (Botta and Bada 2002; Elsila et al. 2016).

It has also been hypothesized that the extent to which meteorite parent

71 bodies have undergone aqueous alteration may correspond to observed L-
72 enantiomeric excesses of extraterrestrial amino acids (Glavin and Dworkin 2009).
73 Many amino acids possess a property known as chirality, whereby the chemical
74 compound is composed of two non-superimposable mirror-image structures, or
75 enantiomers. These enantiomers are distinguished as the so-called L-amino acids
76 (“left-handed’’) or D-amino acids (“right-handed”). Terrestrial life uses L-enantiomers
77 almost exclusively as a component of proteins, whereas abiotically synthesized
78 amino acids contain an equal (racemic) mixture of both enantiomers, unless biology
79 or special conditions are used to induce asymmetry. Therefore, chirality is a critical
80 chemical property to monitor when assessing the origins of potential biomolecules.
81 An example of a meteoritic amino acid that is a useful target analyte to
82 evaluate for potential enantiomeric excesses is the non-proteinogenic amino acid
83 isovaline, which is rare in the terrestrial biosphere (Pizzarello et al. 2003; Elsila et al.
84 2011). Different laboratories have reported that isovaline has various L-enantiomeric
85 excesses ranging from 0 % to ~20 %, with an increase in L-enantiomeric excess
86 roughly correlating with an increased degree of aqueous alteration among the
87 carbonaceous chondrites analyzed (Elsila et al. 2016 and references therein). More
88 specifically, unaltered CM and CR type 3 (petrologic type ≥ 2.6, see discussion
89 below) carbonaceous chondrites show racemic isovaline, but more aqueously

altered type1 or type 2 carbonaceous chondrites (petrologic type 2.0 to 2.5, see discussion below) contain L-isovaline excesses (Glavin and Dworkin 2009; Glavin et al. 2010, 2020b; Martins et al. 2015).

Although aliphatic amino acids have been thoroughly investigated in carbonaceous chondrites, hydroxyl (–OH) group-bearing amino acids known as hydroxy amino acids (HAAs) have been understudied except for serine and threonine, which are common proteinogenic amino acids. Koga and Naraoka (2017) revealed the distribution of HAAs in extracts of the Murchison meteorite, including nine newly identified C_3 and C_4 HAAs with α-, β-, and γ-amino group positions (Fig. 1). It is worth noting that HAAs were detected not only in the acid hydrolysates of the hot water extracts, but were also present at comparable or greater abundances in the 6 M HCl extracts of the meteorite residues that had previously experienced hot water extraction (Koga and Naraoka 2017).

There have been limited efforts to detect and quantify amino acids in aqueous HCl extracts of meteorites (Engel and Nagy 1982; Bada et al. 1998; Glavin et al. 1999, Koga and Naraoka 2017). However, those few explorations have yielded intriguing results. For example, Glavin et al. 1999 reported that HCl extraction of chondrites resulted in decreased amino acid abundances compared to the same samples being treated by hot water extraction followed by acid hydrolysis. It was

proposed that this decreased amino acid abundance may be partially explained by potential amino acid degradation processes that might have occurred during HCl extraction (Glavin et al., 1999). Details pertaining to such representative HCl extraction procedures are provided elsewhere (Bada et al., 1998, Glavin et al., 1999). Additionally, what has been learned from investigating the aqueous HCl extract of the Murchison meteorite is that HAAs represent a new subclass of meteoritic amino acids that are not necessarily fully released from the meteorite matrix by hot water extraction alone (Koga and Naraoka 2017). However, it remains unknown what abundances and distributions of structural isomers of HAAs exist in carbonaceous chondrites other than the CM2 Murchison meteorite. Moreover, enantiomeric analyses of HAAs by gas chromatography-mass spectrometry (GC-MS) have been sparsely executed in previous studies, except for targeted searches for serine and threonine (Pizzarello et al. 2012). In this study, we developed a new GC-MS method to investigate the abundances of three- and four-carbon (C_3-C_4) HAA structural isomers and the enantiomeric compositions of chiral HAAs in CM and CR chondrites ranging from type 1 to type 2. This approach allows for the evaluation of the molecular distributions and possible formation pathways of HAAs across a range of carbonaceous chondrites that experienced different degrees of parent body alteration.

MATERIALS AND METHODS

Chemicals and Reagents

Commercial standards of HAAs were purchased from various manufacturers as follows: Sigma-Aldrich: D,L-α-methylserine (>99 % purity), D-threonine (>98 % purity), L-threonine (>98 % purity), D,L-*allo*-threonine (>99 % purity), D,L-isoserine (>98 % purity), D,L-homoserine (>99 % purity), D-β-homoserine (>99 % purity), L-β-homoserine (>99 % purity), Tokyo Chemical Industry (TCI): D,L-4-amino-3-hydroxybutanoic acid (4-A-3-HBA) (>98 % purity), Enamine Ltd.: a combined D,L-isothreonine and D,L-*allo*-isothreonine standard (>95 % purity), and Fluka: D,L-serine (>99 % purity). Racemic standards for 3-amino-2-(hydroxymethyl)propanoic acid (3-A-2-HMPA) and 4-amino-2-hydroxybutanoic acid (4-A-2-HBA) were not commercially available, so the following enantiopure standards of these amino acids were purchased from Sigma-Aldrich: D-3-A-2-HMPA (>96 % purity) and L-4-A-2-HBA (>96 % purity). The standard for D,L-α-methylisoserine was obtained by hydrolysis of D,L-methyl-3-amino-2-hydroxy-2-methylpropanoate hydrochloride (>97 % purity, Aurum Pharmatech LLC) via 6 M HCl vapor hydrolysis at 150 °C for 3 h (Glavin et al., 2006). A stock mixed HAA solution (~8 μM per analyte) was prepared by combining individual HAA standards described above in Millipore Integral 10 ultrapure water (18.2 MΩ, <3 ppb total organic carbon). As an internal standard, a

147 stock solution of 8-aminooctanoic acid (8-AOA) (>99 %, Sigma Aldrich) was
148 prepared with the same concentration (~8 μM).

149 All glassware and sample handling tools were rinsed with Millipore Integral
150 10 ultrapure water (18.2 MΩ-cm, ≤ 3 ppb total organic carbon), wrapped in aluminum
151 foil, and heated at 500 °C, in air, overnight to remove organic contamination.
152 Preparation of reagents used to perform acid vapor hydrolysis (Glavin et al. 2006)
153 and desalting by cation exchange chromatography (Glavin et al. 2006; Simkus et al.
154 2019) are described elsewhere. Acid extraction was performed using 6 M doubly
155 distilled HCl (ddHCl). Pre-column derivatization of samples before GC-MS analyses
156 involved the use of acetyl chloride (Acros Organics, 99+ %), isopropanol (Sigma-
157 Aldrich, 99+ %), heptafluorobutyric anhydride (HFBA, Sigma-Aldrich, ≥98 %), and
158 chloroform (Sigma-Aldrich, for HPLC, ≥99.9 %).

159 **Meteorite Samples and Sample Preparation**

160 The interior chips of five CM and four CR chondrites, none of which
161 contained visible evidence of fusion crust, were used for HAA analyses in this study
162 (Table 1). The Antarctic CM2 chondrites: Asuka 881458 (A-881458) and Yamato
163 791198 (Y-791198), were provided by the Antarctic meteorite curator at the National
164 Institute of Polar Research (NIPR) in Tokyo, Japan. All other meteorites, including
165 the other Antarctic CM2 chondrites: Lewis Cliffs (LEW) 90500 and Lonewolf

166 Nunataks (LON) 94101, the CM 1/2 chondrite: Allan Hills (ALH) 83100, the CR2
167 chondrites: Miller Range (MIL) 07525, Meteorite Hills (MET) 00426 and LaPaz
168 Icefield (LAP) 02342, and the CR1 chondrite: Grosvenor Mountains (GRO) 95577
169 were provided by the Antarctic meteorite curator at the NASA Johnson Space
170 Center. The petrologic subtype assignments of these carbonaceous chondrites were
171 suggested by several previous studies, as summarized in Table 1. In this study, the
172 CR chondrite subtype classifications were based on the alteration metrics proposed
173 by Harju et al. (2014), Howard et al. (2015), and Alexander et al. (2013). The CM
174 chondrite subtype classifications that were available in the literature and used in
175 Table 1, were based on the aqueous alteration metrics described by Rubin et al.
176 (2007), Howard et al. (2015) and Alexander et al. (2013). Although the subtype for A-
177 881458 was not available, this meteorite has been classified as a weakly heated
178 CM2 chondrite (Nakamura 2005; Kimura et al. 2011).
179 Each meteorite chip was separately crushed into a fine powder using
180 ceramic mortars and pestles inside a positive pressure ISO 5 HEPA filtered laminar
181 flow hood. A portion of each powdered sample (mass ~ 0.14 – 0.36 g, Table 1) was
182 flame-sealed separately in a glass ampoule with 1 mL of ultrapure water and
183 extracted at 100 °C for 24 h (hereafter referred to as “Hot Water (HW) extraction”).
184 Following HW extraction, the supernatants were separated from the residues and

185 half of the HW extract supernatants were subjected to a 6 M ddHCl vapor hydrolysis
186 procedure at 150 °C for 3 h to determine total hydrolyzable amino acid content
187 (Glavin et al. 2006). The acid hydrolyzed HW extracts were then dried under vacuum
188 to remove excess HCl. The residues that remained after completing the HW
189 extraction were then subjected to a second extraction procedure using 6 M ddHCl at
190 105 °C for 24 h (hereafter referred to as “HCl extraction”). The HCl extraction
191 supernatants were then dried to a residue and set aside until further processing.

192 Once the supernatants from both extraction procedures were dried to a
193 residue, each residue was individually reconstituted in 1 mL of ultrapure water before
194 being desalted using cation-exchange chromatography. The reconstituted HW and
195 HCl extracts were individually loaded onto separate AG 50W-X8, 100-200 mesh,
196 hydrogen form cation-exchange chromatography columns and desalted as described
197 in Simkus et al. (2019). The resultant desalted HW and HCl extract eluates were
198 dried and reconstituted in 100 µL of ultrapure water. Next, 30 µL of each re-
199 suspended meteorite extract and the HAA standard solution, were separately spiked
200 with 10 µL of the internal standard (8-AOA) before being dried and derivatized for
201 HAA analyses using the following protocol: 1) esterification with 160 µL of
202 isopropanol and 40 µL of acetyl chloride at 100 °C for 3 h, 2) acylation with 50 µL of
203 HFBA at 100 °C for 3 h, 3) removal of excess heptafluorobutyric acids using a

stream of dry nitrogen, and 4) dissolution into 10 μL of chloroform before injection into the GC-MS system for analysis. Procedural blanks composed of ultrapure water were prepared in parallel using the identical extraction and processing protocols as the meteorite samples were subjected to, and the procedural blanks were analyzed to provide background-corrected abundance estimates of target analytes.

GC-MS Analysis

The HW and HCl extracts of the CM and CR chondrites were analyzed for HAA abundances, distributions, and enantiomeric ratios by GC-MS. The HFBA-isopropyl derivatives of HAAs were analyzed using a Thermo Trace GC and Thermo DSQII electron-impact quadrupole mass spectrometer. Chromatographic separation was achieved using a 5 m base-deactivated fused silica guard column (Restek) in series with two 25 m CP-Chirasil-Dex CB columns (Agilent), followed by two 25 m Chirasil L-Val columns (Agilent). A helium flow rate of 2.6 mL/min, and the following temperature program was employed during chromatographic separation: initial oven temperature was 60 °C and was held for 2 min, followed by ramping at 20 °C/min to 75 °C and held for 40 min, followed by ramping at 20 °C/min to 120 °C, followed by ramping at 1 °C/min to 130 °C, and finally ramping at 3 °C/min to 200 °C and held for 2 min.

The use of two optically active stationary phases in series order of CP-Chirasil-Dex CB and Chirasil L-Val (each 50 m length) is a significant improvement of the GC-MS method used in this study to achieve chromatographic separations of structural isomers and enantiomers of HAAs, compared to previous work (Koga and Naraoka, 2017). Other significant improvements include optimization of the derivatization conditions (reagents, reaction temperatures, and durations) and the GC heating program. Furthermore, the GC-MS method was optimized to separate the enantiomers of α-methylserine, an amino acid with the same α-dialkyl structure as isovaline, which has been observed to possess L-enantiomeric excesses in other meteorites (Elsila et al. 2016 and references therein). Hydroxy amino acids in carbonaceous chondrites were identified based on retention times and mass fragmentation patterns compared to those of commercial standards. To improve instrumental detection limits, we operated the mass spectrometer in single ion monitoring mode to observe the characteristic HAA fragment ions for each analyte. Quantification was performed using the fragment ions of a given analyte that did not experience coelution with potentially interfering ions when analyzing a given sample. This approach helped to improve the accuracy of the quantified measurements reported here. Hence, depending on the presence of interfering ions, in many cases different fragment ions were used to quantify the same HAAs in different meteorite

241 samples (*e.g.*, *m/z* 252 and *m/z* 466 for D,L-α-methylisoserine). A detailed overview
242 of which fragment ions were selected for quantifying a given analyte in each sample
243 is provided in Table S1. HAAs were quantified by comparing the procedural blank-
244 subtracted mass chromatographic peak areas in the meteorite samples to those in
245 the analytical standard analyzed on the same day. The HAA peak areas obtained
246 from the meteorite samples, blanks, and standards were corrected based on the
247 associated peak area of the 8-aminooctanoic acid internal standard in an effort to
248 minimize analytical errors between GC-MS analyses that were executed using
249 different injection volumes (typical injection volumes ranged from 1–3 μL).

250 **RESULTS AND DISCUSSION**

251 **The Analytical Performance of the Developed Method**

252 Figures 2 and 3 show the extracted ion chromatograms of the HAA
253 derivatives obtained from the HW and HCl extracts of each meteorite, the procedural
254 blanks, and an HAA standard. Most target chiral HAAs were enantiomerically
255 resolved by this GC-MS method, except for α-methylisoserine and β-homoserine
256 (Fig. 2 and 3). Although some chromatographic resolution was achieved for D,L-
257 isoserine, these peaks were not baseline-resolved. The enantiomers of isothreonine
258 and *allo*-isothreonine were successfully separated by the developed method;
259 however, the elution orders of the enantiomers for these species were not

260 determined due to the lack of enantiopure standards.

261 Although chromatographic resolution of HAA structural isomers was
262 achieved among the analytes in the HAA standard, select instances of coelution
263 were observed between target HAA species and non-targeted, non-HAA species in
264 some meteorites due to the chemical complexities of the samples studied here. Non-
265 proteinogenic C_4 HAAs were not detected in the procedural blank; however, trace
266 quantities of the common biological contaminants, L-serine and L-threonine, were
267 identified in the procedural blank. The abundances of L-serine and L-threonine in the
268 procedural blank were subtracted when performing quantification analyses of these
269 species in the meteorite extracts. Many of the targeted C_3 and C_4 HAAs were
270 detected in both the HW and HCl extracts, including α-methylisoserine, which had
271 not previously been identified in meteorites due to the lack of a commercially
272 available standard (Koga and Naraoka 2017).

273 **Hydroxy Amino Acid Abundances**

274 The distributions and abundances of HAAs observed in the HW and HCl
275 extracts of the CM chondrites are shown in Table 2. The total HAA content in each
276 extract of the CM chondrites ranged from 2.43 ± 0.09 nmol/g in the HCl extract of
277 ALH 83100 (CM1/2) to 74 ± 5 nmol/g in the HCl extract of Y-791198 (CM2). The
278 trend of combined HAA abundances in the two extracts (HW + HCl extracts) of CM

279 chondrites follows the order of Y-791198 (CM2), 126 ± 5 nmol/g > A-881458 (CM2),
280 15.2 ± 0.3 nmol/g > ALH 83100 (CM1/2), 9.8 ± 0.2 nmol/g > LON 94101 (CM2), 7.0 ±
281 0.5 nmol/g ≈ LEW 90500 (CM2), 6.94 ± 0.09 nmol/g. It must be noted that the HW
282 extract of ALH 83100 contained elevated abundances of L-serine (5.0 ± 0.2 nmol/g)
283 and L-threonine (1.66 ± 0.06 nmol/g) relative to the total HAA abundances (7.4 ± 0.2
284 nmol/g). Consequently, the HW extract of ALH 83100 likely contained significant
285 terrestrial contamination of L-serine and L-threonine. A similar L- serine
286 contamination was observed for the HCl extract of LON 94101 (L-serine: 2.1 ± 0.5
287 nmol/g, total abundance: 4.5 ± 0.5 nmol/g). If these likely L-contaminants are
288 excluded from the total HAA sum, the observed trend in total HAA abundances would
289 appear to be correlated with the phyllosilicate fraction subtype of the CM chondrites
290 (Howard et al. 2015) (*i.e.*, CM1.6 Y-791198 > CM1.4 LEW 90500 > CM1.3 LON
291 94101 > CM1.2 ALH 83100 (Table1), not included in this trend is A-881458 because
292 this meteorite was not investigated in Howard et al. (2015)).
293 For the CR chondrites, total HAA content in each extract ranged from 0.42 ±
294 0.01 nmol/g for the HW extract of GRO 95577 (CR1) to 171 ± 1 nmol/g for the HW
295 extract of MIL 07525 (CR2) (Table 3). The trend of combined HAA abundances in the
296 two extracts (HW + HCl extracts) of CR chondrites followed the order of MIL 07525
297 (CR2), 315 ± 6 nmol/g > MET 00426 (CR2), 270 ± 10 nmol/g > LAP 02342 (CR2),

298 200 ± 10 nmol/g > GRO 95577 (CR1), 10 ± 1 nmol/g. This trend is generally
299 correlated with the subtype based on the degree of hydration (wt% H in water and
300 OH) of the CR carbonaceous chondrites (Alexander et al. 2013) (*i.e.*, CR2.6 MET
301 00426 > CR 2.5 LAP 02342 > CR1.3 GRO 95577 (Table 1), not included in this trend
302 is MIL 07525, which was not investigated by Alexander et al. (2013)).

303 Interestingly the CR2 chondrites (MIL 07525, LAP 02342, and MET 00426)
304 contained greater abundances of the individual HAAs, serine and α-methylserine,
305 when summed from their respective HW + HCl extracts, than any other α-HAA
306 detected in the summed HW + HCl extracts of any of the CM or CR meteorites
307 (Table 4). The total abundances of α-HAAs was higher in the CR2 chondrites
308 compared to the CM2 chondrites. In contrast to this disparity among α-HAAs, the
309 abundances of β- and γ-HAAs in CR chondrites were within a similar range to those
310 in CM chondrites. For example, the combined β-HAA abundances in the two extracts
311 of each CR chondrite ranged from 0.82 ± 0.01 nmol/g for GRO 95577 to 18.4 ± 0.6
312 nmol/g for MIL 07525, while those of CM chondrites ranged from 0.69 ± 0.02 nmol/g
313 for ALH 83100 to 37.1 ± 0.9 nmol/g for Y-791198. Likewise, the combined γ-HAA
314 abundances in the two extracts of each CR chondrite ranged from 0.112 ± 0.005
315 nmol/g for GRO 95577 to 1.3 ± 0.1 nmol/g for MIL 07525, while those of CM
316 chondrites ranged from 0.098 ± 0.002 nmol/g for ALH 83100 to 3.14 ± 0.09 nmol/g

317 for Y-791198. This marks the first reporting of disparities between total abundances
318 of α-HAAs compared to β- and γ-HAAs in CM and CR chondrites, possibly indicating
319 that varying formation pathways may be responsible for the observed differences.
320 It is also worth noting that for all CR2 meteorites and most of the CMs
321 studied here, the HCl extracts are the only ones that contain γ-HAAs (Tables 2 and
322 3). It is possible that an exposure of γ-HAA precursors in the meteorite matrix to HCl
323 during the extraction process might induce the formation or liberation of γ-HAAs, or
324 their precursors to allow synthesis during workup. Further work is needed to
325 investigate whether a discrepancy among structural amino acid isomer distributions
326 between HW and HCl extracts would also be observed for conventional amino acids
327 (*e.g.,* C_5 amino acid isomers, as investigated in previous works (Elsila et al. 2016
328 and references therein)).
329 Figures 4A and 4B show the relative abundances of C_3 and C_4 HAAs in the
330 HW and HCl extracts, respectively, as a function of amine position (α-, β-, or γ-)
331 relative to the total abundance of C_3 and C_4 HAAs. The relative abundances were
332 calculated from the data in Tables 2 and 3. The relative abundances of α-HAAs were
333 larger than those of β-HAAs and γ-HAAs for the HW and HCl extracts of all CM and
334 CR chondrites (Fig. 4A and 4B). It must be noted that the relative abundances in the
335 HW extract of ALH 83100 and the HCl extract of GRO 95577 were biased toward α-

336 HAA isomers by relatively significant L-serine and L-threonine abundances that were
337 likely due to terrestrial contamination (see Tables 2 and 3). For each meteorite, the
338 relative abundance of β-HAAs in the HCl extract were comparable to, or greater
339 than, that in the respective HW extract, except for LON 94101 and GRO 95577 (Fig.
340 4A and 4B). Similarly, the relative abundances of γ-HAAs in the HCl extract of each
341 meteorite were comparable to, or greater than, that in the respective HW extract,
342 except for GRO 95577. The observed difference in relative abundances between the
343 HW extract of CR1 GRO 95577 and all the other extracts of all the other CRs studied
344 here is intriguing. Further work is needed to determine the origins of this difference,
345 but that is beyond the scope of the present study.

346 Figure 4C shows the relative HAA abundances in the combined (HW + HCl)
347 extracts of CM and CR chondrites as a function of amine position (α-, β-, or γ-). The
348 α-HAA isomers dominate the distribution of C_3 and C_4 HAA isomers for all
349 meteorites. In particular, the CR2 chondrites (MIL 07525, LAP 02342, and MET
350 00426) showed larger relative abundances of α-HAA isomers than β- or γ-HAA
351 isomers, mainly deriving from abundant serine and α-methylserine (see Table 3). In
352 contrast, the CM2 chondrites (Y-791198, A-881458, LEW 90500, and LON 94101)
353 possessed noticeably greater relative abundances of β- and γ-HAAs than the CR
354 chondrites studied here. The disparities between the relative abundances of α-HAAs

355 compared to β- and γ-HAAs in the CM2 and CR chondrites might suggest that
356 different HAA formation, and/or preservation, mechanisms occurred in CM and CR
357 chondrite parent bodies.

358 **Enantiomeric Compositions of Non-Proteinogenic Hydroxy Amino Acids**

359 Since α-dialkyl amino acids, such as isovaline, have been targeted in
360 previous meteorite studies to evaluate their enantiomeric excesses in meteorites,
361 given their resistances to racemization (Pollock et al. 1975), a similar α-dialkyl amino
362 acid, α-methylserine, was targeted in this study to explore its possible enantiomeric
363 excess in meteorites. We first resolved D,L-α-methylserine in carbonaceous
364 chondrites using the developed GC-MS method (Fig. 2 and 3). However, it was
365 found that α-methylserine was racemic within error in most carbonaceous chondrite
366 extracts (Table 5). Thus, the α-methylserine in CM and CR chondrites did not appear
367 to show convincing L-enantiomeric excesses correlating with the degree of aqueous
368 alteration, a phenomenon observed in isovaline (Elsila et al. 2016 and references
369 therein; Glavin et al. 2020a,b).

370 The notable exceptions to this observation of racemic α-methylserine
371 included the HCl extracts of LEW 90500 and MET 00426, and the HW extracts of
372 LON 094101 and MIL 07525. These extracts of LEW 90500 and LON 094101
373 contained very nearly racemic mixtures of α-methylserine that were slightly L-

374 enantiomerically enriched, outside of the measurement error, as they exhibited α-
375 methylserine L-enantiomeric excesses of 2.4 ± 0.8 % and 1.9 ± 0.6 %, respectively
376 (Table 5). The aforementioned extracts of MIL 07525 and MET 00426 showed slight
377 D-α-methylserine enantiomeric enrichments outside of errors, as they exhibited α-
378 methylserine L-enantiomeric excesses of -5.4 ± 0.8 % and -6.6 ± 0.8 %, respectively
379 (Table 5). These narrow L- or D-α-methylserine enantiomeric excesses observed
380 outside of errors are anomalous compared to the α-methylserine data collected from
381 most other meteorite extracts analyzed here. They are also inconsistent with the
382 findings from their respective HW or HCl extract counterparts for the same samples,
383 which showed α-methylserine was racemic. Future quantitative analyses are
384 necessary to determine if these anomalies are similarly observed by alternative
385 analytical methodologies, such as ultraperformance liquid chromatography with
386 fluorescence detection and time-of-flight mass spectrometry (UPLC-FD/ToF-MS)
387 (Glavin et al., 2020b).

388 The other non-proteinogenic α-HAAs, namely *allo*-threonine and
389 homoserine, were affected by coelution with interfering species in most of the
390 carbonaceous chondrites we studied, which made accurate quantification of their
391 enantiomers not possible (Fig. 2 and Fig. 3). Some meteorite extracts showed the
392 chromatographic peaks of *allo*-threonine and homoserine without coelution. In these

393 cases, *allo*-threonine and homoserine were racemic within analytical errors, except
394 for homoserine in ALH 83100 (Table 5). The L-enantiomeric excess for homoserine
395 observed in the HW and HCl extracts of ALH 83100 were 51.7 ± 1.2 % and 8.0 ± 1.6
396 %, respectively (Table 5). However, it should be noted that L-homoserine can be
397 produced by methionine metabolism as a terrestrial biological component (Matsuo
398 and Greenberg 1955). Furthermore, in this study, we observed relatively significant
399 abundances of L-serine and L-threonine in both extracts of ALH 83100, which were
400 terrestrial contamination (Table 2). Thus, it is plausible that the L-enantiomeric
401 excesses of homoserine in the HW and HCl extracts of ALH 83100 could also be
402 derived from terrestrial contamination. Future isotopic measurements will be required
403 to determine the origin of the L-homoserine enantiomeric excesses in ALH 83100.

404 **A Proposed Formation Mechanism for Prominent α-Hydroxy Amino Acids:**
405 **Strecker Cyanohydrin Synthesis**

406 This study revealed that α-methylserine and serine were significantly more
407 abundant in the combined (HW + HCl) extracts of CR2 chondrites (LAP 02342, MET
408 00426, and MIL 07525) than other α-HAAs, such as threonine, *allo*-threonine, and
409 homoserine (Table 4). These large abundances of serine and α-methylserine may be
410 explained by the predominance of the Strecker cyanohydrin synthesis within the
411 parent bodies of the CR chondrites during the aqueous alteration phase, as has

412 been proposed to explain the presence of other α-amino acids in meteorite samples
413 (Peltzer and Bada, 1978; Peltzer et al., 1984; Lerner et al., 1993; Glavin et al. 2010).
414 The predominance of α-methylserine and serine compared to other α-HAAs could be
415 used to make inferences about the relative abundances of α-HAA precursors in CR
416 chondrite parent bodies that could have been more significantly incorporated into the
417 Strecker cyanohydrin synthesis to generate their respective HAAs. In particular,
418 inferences could be made about the potential for elevated relative abundances of
419 possible carbonyl-containing precursors of α-methylserine (hydroxyacetone), serine
420 (glycolaldehyde), threonine and/or *allo*-threonine (lactaldehyde), and homoserine (3-
421 hydroxypropanal), as illustrated in the proposed Strecker cyanohydrin formation
422 mechanisms shown in Fig. 5.
423 One critical aspect of the Strecker cyanohydrin synthesis that could have
424 also contributed to elevated abundances of α-methylserine and serine in the extracts
425 of the CR2 chondrites studied here is the abundance of ammonia in the CR
426 meteorite parent bodies. It has been reported that CR2 chondrites were enriched in
427 ammonia, and that ammonia was present not only in the free form but also in a
428 bound form that can be released from insoluble organic matter by hydrothermal
429 treatment (Pizzarello and Holmes 2009; Pizzarello et al. 2011). This finding suggests
430 that parent body environments of CR2 chondrites may have contained elevated

abundances of ammonia. In such ammonia-enriched environments, the Strecker cyanohydrin synthesis (see Fig. 5 for examples) could have proceeded by forming an imine from a precursor aldehyde or ketone, in the presence of ammonia. The imine could then react with HCN to form an aminonitrile that becomes hydrolyzed to yield an α-amino acid (Peltzer and Bada, 1978; Peltzer et al., 1984). However, in ammonia-depleted environments, the Strecker cyanohydrin synthesis would be more likely to proceed by forming a cyanohydrin, as opposed to an aminonitrile, where the cyanohydrin could subsequently be hydrolyzed to yield an α-hydroxy acid (Peltzer and Bada, 1978; Peltzer et al., 1984). Pizzarello et al. (2010) reported that the CM2 Murchison meteorite contained a lower abundance ratio of α-amino acids to α-hydroxy acids (~1.3) than that of CR2 chondrites (8.0 for GRA 95229 and 16.0 for LAP 02342). The ammonia concentration in the Murchison meteorite was an order of magnitude smaller than those of the CR2 chondrites, 1.1–1.3 μmol/g (Pizzarello et al. 1994) and 14.1–18.9 μmol/g (Pizzarello and Holmes 2009), respectively. Thus, the observations may suggest that relatively ammonia-depleted environments (*e.g.,* CM chondrite parent bodies similar to Murchison meteorite) favored the synthesis of α-hydroxy acids by the cyanohydrin synthesis compared to the relatively ammonia-rich environments (*e.g.,* CR chondrite parent bodies similar to GRA 95229 and LAP 02342). Further ammonia quantifications in CM- and CR-type chondrites are needed

450 to fully understand the synthetic reigns for the synthesis of meteoritic hydroxy acids
451 and amino acids. In this work, the CM2 chondrites (Y-791198, A-881458, LEW
452 90500, and LON 94101) were found to contain smaller relative abundances of α-
453 HAAs than the CR2 chondrites (MIL 07525, LAP 02342, and MET 00426) (Fig. 4C).
454 One possible explanation for this observation could be the existence of differences in
455 ammonia concentrations in the CR and CM chondrite parent bodies studied here.
456 However, it is also possible that other factors may have contributed to this observed
457 disparity. For example, different parent bodies could have evolved at dissimilar times
458 and in disparate locations, resulting in varying synthetic yields of α-HAAs.
459 Additionally, it is possible that α-HAAs could have been formed elsewhere in the
460 interstellar medium prior to incorporation into meteorite parent body environments.
461 For example, several laboratory experiments have revealed that the ultraviolet
462 photolysis of interstellar ice analogs can yield the α-HAA, serine (Bernstein et al.
463 2002; Muñoz Caro et al. 2002; Elsila et al. 2007; Oba et al. 2016). Nonetheless, the
464 observation of greater α-HAA relative abundances in the CR2 extracts than the CM2
465 extracts analyzed here is an intriguing result that warrants further investigation to
466 determine the genesis of this difference.

A Proposed Formation Mechanism for β-, and γ-Hydroxy Amino Acids: Ammonia-Involved Formose-like Reaction

Previous reports suggest that the Strecker cyanohydrin synthesis can form α-amino acids, but not β- and γ-amino acids (Elsila et al. 2012 and references therein). Consequently, to explain the distribution of HAA structural isomers observed in the carbonaceous chondrites studied here, a complementary formation mechanism is required. The syntheses of α-, β- and γ-HAAs were observed in laboratory experiments performed by Koga and Naraoka (2017), which produced a total of 17 amino acids via a formose-like reaction involving formaldehyde, acetaldehyde, glycolaldehyde, and ammonia in aqueous solution at 60 °C for 6 days. Therefore, insight into how structural diversity of HAAs may have been formed in the parent bodies of the meteorites analyzed in this study may be gleaned from a combination of the experiments outlined in Koga and Naraoka (2017) and the formose reaction. In the formose reaction, glycolaldehyde, and eventually sugars, are formed from the condensation of formaldehyde molecules in alkaline solution (Breslow 1959). It has been proposed that the formation of β- and γ-HAAs may follow a similar line of synthesis, whereby aldehydes (*e.g.,* formaldehyde and glycolaldehyde), in the presence of ammonia, could yield amino acids via the formose reaction and an aldol condensation (Koga and Naraoka 2017). The

nomenclature for such a formation pathway for β- and γ-HAAs could be considered an ammonia-involved formose-like reaction. Therefore, the presence of β- and γ-HAA isomers found in all the carbonaceous chondrites analyzed in this work suggests that an ammonia-involved formose-like reaction may have occurred in the parent bodies of the meteorites studied here, which could have complemented the Strecker cyanohydrin synthesis to generate HAA structural diversity. The more predominant relative abundances of β- and γ-HAAs in CM chondrites (Fig. 4C) may also suggest that a formose-like reaction could have occurred more prominently in the parent bodies of CM chondrites than CR chondrites. It is worth noting that α-amino acids could be generated not only by the Strecker cyanohydrin reaction, but also by an ammonia-involved formose-like reaction since laboratory experiments conducted by Koga and Naraoka (2017) and Kebukawa et al. (2017) observed the formation of various α-amino acids from aldehydes and ammonia.

A similar reaction to an ammonia-involved formose-like reaction has been recognized to produce chondritic insoluble organic matter, such as organic solids (Kebukawa et al. 2013) and various soluble organic compounds, including N-bearing compounds (Kebukawa et al. 2020) and conventional amino acids other than HAAs (Kebukawa et al. 2017). The recent discovery of hexamethylenetetramine (HMT), and hydroxy- and hydroxymethyl- variants of HMT in CM2 meteorites (Oba et al.

505 2020) may suggest a relationship to facilitate an ammonia-involved formose-like
506 reaction. Further studies to look for HMT and its variants in CR meteorites could be
507 illuminating.

508 While the Strecker cyanohydrin reaction utilizes aldehydes (or ketones),
509 ammonia, and cyanide to synthesize only α-amino acids, an ammonia-involved
510 formose-like reaction requires only aldehydes and ammonia, but not cyanide, to
511 produce α-, β-, and γ-HAAs. Thus, both formation mechanisms could have occurred
512 simultaneously using the same pool of starting reagents (*i.e.,* aldehydes and
513 ammonia), whereas cyanide concentrations in meteorite parent bodies would
514 influence which reaction predominated. For the Strecker cyanohydrin synthesis to
515 have predominated, the parent body environment would have needed cyanide-rich
516 conditions, which also include precursor aldehydes and/or ketones and ammonia to
517 facilitate the formation of α-HAAs. Over time, HCN abundances on the parent bodies
518 could have become depleted due to consumption via the Strecker cyanohydrin
519 reaction, HCN polymerization (Lerner et al. 1993), and metal-cyanide complexation
520 (Smith et al. 2019). Such HCN-poor environments may have been unfavorable for
521 the viability of the Strecker cyanohydrin synthesis to produce α-HAAs. However, an
522 ammonia-involved formose-like reaction occurs readily in cyanide-depleted
523 scenarios to produce a mixture of α-, β-, and γ-HAAs from aldehydes and ammonia

524 (Koga and Naraoka, 2017). Therefore, the depletion of HCN on the meteorite parent
525 bodies may have marked the transition from α-HAA production with relatively
526 enhanced contributions by the Strecker cyanohydrin synthesis to the formation of α-,
527 β-, and γ-HAAs with relatively large contributions from an ammonia-involved
528 formose-like reaction. In the future, laboratory experiments that simulate the
529 conditions of the parent bodies of CM and CR chondrites, while using aldehydes,
530 ammonia, and ^{13}C-labeled HCN, will be needed to better evaluate the relative
531 contributions to HAA syntheses of the Strecker cyanohydrin reaction and an
532 ammonia-involved formose-like reaction.

533 HAA analyses conducted in this study revealed that the relative abundances
534 of β- and γ-HAAs in the HCl extracts were comparable to, or greater than those in
535 the HW extracts for most CM and CR chondrites (Fig. 4A and 4B). This observation
536 may indicate that HCl extracted β- and γ-HAAs more efficiently than HW.
537 Alternatively, it is not known whether the exposure of the meteorite sample to the
538 HW extraction produces more α-HAAs from α-HAA precursors, or likewise for HCl
539 exposure producing more β- and γ-HAAs from β- and γ-HAA precursors. One
540 possible group or precursor compounds of β- and γ-HAAs is hydroxy lactams.
541 Cooper and Cronin (1995) reported an extensive homologous series of lactams in
542 the CM2 Murchison meteorite, suggesting that hydroxy lactams could be present in

carbonaceous chondrites. In future works, the measurement of HAAs' isotopic compositions of the HW and HCl extracts are necessary to more rigorously evaluate whether solubility or synthetic considerations can explain the observed differences.

CONCLUSIONS

The research presented here entailed the analyses of five CM chondrites and four CR chondrites to examine the abundances, distributions, and enantiomeric ratios of a suite of HAAs in the HW and 6 M HCl extracts of these chondrites. To perform the necessary HAA analyses, we developed a new GC-MS analytical technique to target thirteen HAAs, including α-, β-, and γ-HAAs.

The HAA analyses performed in this study revealed that distinct differences in α-HAA distributions existed between CR and CM chondrites, which are groups of chondrites with different chemistries. Elevated abundances of the α-hydroxy amino acids serine and α-methylserine were observed more prominently in the CR2 chondrites than the CM chondrites. In contrast to disproportionate α-HAA abundance comparisons between the chondrites studied here, total abundances of β- and γ-HAAs were similar between the CM and CR chondrites. The total HAA abundances of the CM and CR chondrites generally appeared to be inversely proportional to the degree of aqueous alteration in the parent bodies, as determined by the phyllosilicate fraction (Howard et al., 2015) for CM chondrites and the degree of

562 hydration (Alexander et al. 2013) for CR chondrites, respectively. However, it is worth
563 noting that A-881458 and MIL 07525 are not necessarily included in this assessment
564 as these two chondrites do not currently possess a phyllosilicate fraction
565 classification, nor a degree of hydration assessment. The chondrite ALH 83100 is
566 also not included in this assessment due to the likely significant L-serine and L-
567 threonine contamination observed, skewing the total HAA abundance observed for
568 this meteorite. A plurality of non-proteinogenic HAAs, including α-methylserine, did
569 not show enantiomeric excesses correlating with the degree of the aqueous
570 alteration, a phenomenon previously observed in meteoritic isovaline (Glavin and
571 Dworkin, 2009). Further investigations are needed to verify observed enantiomeric
572 excesses of α-methylserine and homoserine in select carbonaceous chondrite
573 extracts with quantitative analyses using UPLC-FD/ToF-MS and isotopic analyses
574 using gas chromatography-combustion-isotope ratio mass spectrometry.

575 The elevated total abundances of α-HAAs in CR2 chondrites could be
576 produced by the Strecker cyanohydrin reaction, which may dominate under
577 ammonia-enriched conditions in the meteorite parent body, as suggested by
578 Pizzarello et al. (2011). The ubiquitous presence of β- and γ-HAAs in CM and CR
579 chondrites, but more predominantly in the CM chondrites studied here, might
580 suggest that a process similar to an ammonia-involved formose-like reaction

proceeded in the meteorite parent bodies, and perhaps more so in the parent bodies of CM chondrites (Koga and Naraoka 2017) than CR chondrites. Meteoritic α-HAAs could be generated not only by the Strecker cyanohydrin reaction, but also an ammonia-involved formose-like reaction. Further investigations are needed to confirm the extent to which these formation mechanisms are responsible for the HAA abundances observed in the meteorite extracts analyzed here.

ACKNOWLEDGEMENTS

This work was supported by the JSPS Overseas Challenge Program for Young Researchers Grant (number 201880018), the NASA Astrobiology Institute through award 13-13NAI7-0032 to the Goddard Center for Astrobiology, and a grant from the Simons Foundation (SCOL award 302497 to J.P.D.). We thank the National Institute of Polar Research and the Antarctic meteorite curator at the NASA Johnson Space Center for providing the meteorite samples used in this study. US Antarctic meteorite samples were recovered by the Antarctic Search for Meteorites (ANSMET) program which has been funded by NSF and NASA and characterized and curated by the Department of Mineral Sciences of the Smithsonian Institution and the Astromaterials Curation Office at the NASA Johnson Space Center. Japanese Antarctic meteorite samples were provided by the National Institute of Polar Research (NIPR). We

599 appreciate valuable comments on the manuscript from two anonymous reviewers.

600 The authors declare no conflicts of interest.

601 **REFERENCES**

602 Alexander C. M. O. D., Howard K. T., Bowden R., and Fogel M. L. 2013. The
603 classification of CM and CR chondrites using bulk H, C and N abundances and
604 isotopic compositions. *Geochimica et Cosmochimica Acta* 123:244–260.
605 Bada J. L., Glavin D. P., McDonald G. D., and Becker L. 1998. A Search for
606 Endogenous Amino Acids in Martian Meteorite ALH84001. *Science* 279:362–
607 365.
608 Bernstein M. P., Dworkin J. P., Sandford S. A., Cooper G. W., and Allamandola L. J.
609 2002. Racemic amino acids from the ultraviolet photolysis of interstellar ice
610 analogues. *Nature* 416:401–403.
611 Botta O., and Bada J. L. 2002. Extraterrestrial organic compounds in meteorites.
612 *Surveys in Geophysics* 23:411–467.
613 Breslow R. 1959. On the mechanism of the formose reaction. *Tetrahedron Letters*
614 1:22–26.
615 Burton A. S., Grunsfeld S., Elsila J. E., Glavin D. P., and Dworkin J. P. 2014. The
616 effects of parent-body hydrothermal heating on amino acid abundances in CI-
617 like chondrites. *Polar Science* 8:255–263.
618 Chyba C., and Sagan C. 1992. Endogenous production, exogenous delivery and
619 impact-shock synthesis of organic molecules: an inventory for the origins of life.
620 *Nature* 355:125–132.
621 Cooper G. W., and Cronin J. R. 1995. Linear and cyclic aliphatic carboxamides of the
622 Murchison meteorite: Hydrolyzable derivatives of amino acids and other
623 carboxylic acids. *Geochimica et Cosmochimica Acta* 59:1003–1015.
624 Elsila J. E., Dworkin J. P., Bernstein M. P., Martin M. P., and Sandford S. A. 2007.
625 Mechanisms of Amino Acid Formation in Interstellar Ice Analogs. *The*
626 *Astrophysical Journal* 660:911–918.
627 Elsila J. E., Charnley S. B., Burton A. S., Glavin D. P., and Dworkin J. P. 2012.
628 Compound-specific carbon, nitrogen, and hydrogen isotopic ratios for amino
629 acids in CM and CR chondrites and their use in evaluating potential formation
630 pathways. *Meteoritics and Planetary Science* 47:1517–1536.
631 Elsila J. E., Aponte J. C., Blackmond D. G., Burton A. S., Dworkin J. P., and Glavin D.
632 P. 2016. Meteoritic Amino Acids: Diversity in Compositions Reflects Parent Body
633 Histories. *ACS Central Science* 2:370–379.
634 Engel M. H., and Nagy B. 1982. Distribution and enantiomeric composition of amino
635 acids in the Murchison meteorite. *Nature* 296:837–840.
636 Glavin D. P., Bada J. L., Brinton K. L. F., and McDonald G. D. 1999. Amino acids in
637 the Martian meteorite Nakhla. *Proceedings of the National Academy of Sciences*

96:8835–8838.
Glavin D. P., Dworkin J. P., Aubrey A., Botta O., Doty J. H., Martins Z., and Bada J. L. 2006. Amino acid analyses of Antarctic CM2 meteorites using liquid chromatography-time of flight-mass spectrometry. *Meteoritics and Planetary Science* 41:889–902.
Glavin D. P., and Dworkin J. P. 2009. Enrichment of the amino acid L-isovaline by aqueous alteration on Cl and CM meteorite parent bodies. *Proceedings of the National Academy of Sciences of the United States of America* 106:5487–5492.
Glavin D. P., Callahan M. P., Dworkin J. P., and Elsila J. E. 2010. The effects of parent body processes on amino acids in carbonaceous chondrites. *Meteoritics and Planetary Science* 45:1948–1972.
Glavin D. P., Alexander C. M. O., Aponte J. C., Dworkin J. P., Elsila J. E., and Yabuta H. 2018. *The Origin and Evolution of Organic Matter in Carbonaceous Chondrites and Links to Their Parent Bodies*, Elsevier Inc.
Glavin D. P., Elsila J. E., McLain H. L., Aponte J. C., Parker E. T., Dworkin J. P., Hill D. H., Connolly H. C., and Lauretta D. S. 2020a. Extraterrestrial amino acids and L-enantiomeric excesses in the CM2 carbonaceous chondrites Aguas Zarcas and Murchison. *Meteoritics & Planetary Science* 26:1–26.
Glavin D. P. et al. 2020b. Abundant extraterrestrial amino acids in the primitive CM carbonaceous chondrite Asuka 12236. *Meteoritics & Planetary Science* 28:maps.13560.
Harju E. R., Rubin A. E., Ahn I., Choi B.-G., Ziegler K., and Wasson J. T. 2014. Progressive aqueous alteration of CR carbonaceous chondrites. *Geochimica et Cosmochimica Acta* 139:267–292.
Howard K. T., Alexander C. M. O. D., Schrader D. L., and Dyl K. A. 2015. Classification of hydrous meteorites (CR, CM and C2 ungrouped) by phyllosilicate fraction: PSD-XRD modal mineralogy and planetesimal environments. *Geochimica et Cosmochimica Acta* 149:206–222.
Kebukawa Y., David Kilcoyne A. L., and Cody G. D. 2013. Exploring the potential formation of organic solids in chondrites and comets through polymerization of interstellar formaldehyde. *The Astrophysical Journal* 771:19.
Kebukawa Y., Chan Q. H. S., Tachibana S., Kobayashi K., and Zolensky M. E. 2017. One-pot synthesis of amino acid precursors with insoluble organic matter in planetesimals with aqueous activity. *Science Advances* 3:e1602093.
Kebukawa Y., Nakashima S., Mita H., Muramatsu Y., and Kobayashi K. 2020. Molecular evolution during hydrothermal reactions from formaldehyde and ammonia simulating aqueous alteration in meteorite parent bodies. *Icarus* 347:113827.

676 Kimura M., Grossman J. N., and Weiserg M. K. 2011. Fe-Ni metal and sulfide
677 minerals in CM chondrites: An indicator for thermal history. *Meteoritics &*
678 *Planetary Science* 46:431–442.
679 Koga T., and Naraoka H. 2017. A new family of extraterrestrial amino acids in the
680 Murchison meteorite. *Scientific Reports* 7:1–8.
681 Lerner N. R., Peterson E., and Chang S. 1993. The Strecker synthesis as a source
682 of amino acids in carbonaceous chondrites: Deuterium retention during
683 synthesis. *Geochimica et Cosmochimica Acta* 57:4713–4723.
684 Lerner N. R., and Cooper G. W. 2005. Iminodicarboxylic acids in the Murchison
685 meteorite: Evidence of Strecker reactions. *Geochimica et Cosmochimica Acta*
686 69:2901–2906.
687 Martins Z., Modica P., Zanda B., and D'Hendecourt L. L. S. 2015. The amino acid
688 and hydrocarbon contents of the Paris meteorite: Insights into the most primitive
689 CM chondrite. *Meteoritics & Planetary Science* 50:926–943.
690 Matsuo Y., and Greenberg D. M. 1955. Metabolic formation of homoserine and
691 alpha-aminobutyric acid from methionine. *The Journal of biological chemistry*
692 215:547–54.
693 Muñoz Caro G. M., Meierhenrich U. J., Schutte W. A., Barbier B., Arcones Segovia
694 A., Rosenbauer H., Thiemann W. H. P., Brack A., and Greenberg J. M. 2002.
695 Amino acids from ultraviolet irradiation of interstellar ice analogues. *Nature*
696 416:403–406.
697 Oba Y., Takano Y., Watanabe N., and Kouchi A. 2016. Deuterium Fractionation
698 During Amino Acid Formation By Photolysis of Interstellar Ice Analogs
699 Containing Deuterated Methanol. *The Astrophysical Journal* 827:L18.
700 Peltzer E. T., and Bada J. L. 1978. α-Hydroxycarboxylic acids in the Murchison
701 meteorite. *Nature* 272:443–444.
702 Peltzer E. T., Bada J. L., Schlesinger G., and Miller S. L. 1984. The chemical
703 conditions on the parent body of the murchison meteorite: Some conclusions
704 based on amino, hydroxy and dicarboxylic acids. *Advances in Space Research*
705 4:69–74.
706 Pizzarello S., Feng X., Epstein S., and Cronin J. R. 1994. Isotopic analyses of
707 nitrogenous compounds from the Murchison meteorite: ammonia, amines,
708 amino acids, and polar hydrocarbons. *Geochimica et Cosmochimica Acta*
709 58:5579–5587.
710 Pizzarello S., Zolensky M., and Turk K. A. 2003. Nonracemic isovaline in the
711 Murchison meteorite: Chiral distribution and mineral association. *Geochimica et*
712 *Cosmochimica Acta* 67:1589–1595.
713 Pizzarello S., and Holmes W. 2009. Nitrogen-containing compounds in two CR2

meteorites: 15N composition, molecular distribution and precursor molecules. *Geochimica et Cosmochimica Acta* 73:2150–2162.

Pizzarello S., Wang Y., and Chaban G. M. 2010. A comparative study of the hydroxy acids from the Murchison, GRA 95229 and LAP 02342 meteorites. *Geochimica et Cosmochimica Acta* 74:6206–6217.

Pizzarello S., Williams L. B., Lehman J., Holland G. P., and Yarger J. L. 2011. Abundant ammonia in primitive asteroids and the case for a possible exobiology. *Proceedings of the National Academy of Sciences* 108:4303–4306.

Pizzarello S., Schrader D. L., Monroe A. A., and Lauretta D. S. 2012. Large enantiomeric excesses in primitive meteorites and the diverse effects of water in cosmochemical evolution. *Proceedings of the National Academy of Sciences of the United States of America* 109:11949–11954.

Pollock G. E., Cheng C.-N., Cronin S. E., and Kvenvolden K. A. 1975. Stereoisomers of isovaline in the Murchison meteorite. *Geochimica et Cosmochimica Acta* 39:1571–1573.

Simkus D. N., Aponte J. C., Elsila J. E., Parker E. T., Glavin D. P., and Dworkin J. P. 2019. Methodologies for Analyzing Soluble Organic Compounds in Extraterrestrial Samples: Amino Acids, Amines, Monocarboxylic Acids, Aldehydes, and Ketones. *Life* 9:47.

Smith K. E., House C. H., Arevalo R. D., Dworkin J. P., and Callahan M. P. 2019. Organometallic compounds as carriers of extraterrestrial cyanide in primitive meteorites. *Nature Communications* 10:1–7.

Vollmer C., Pelka M., Leitner J., and Janssen A. 2020. Amorphous silicates as a record of solar nebular and parent body processes—A transmission electron microscope study of fine-grained rims and matrix in three Antarctic CR chondrites. *Meteoritics & Planetary Science* 18:maps.13526.

Figures

α-amino	β-amino	γ-amino
C_3	C_3	
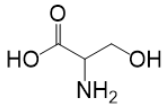 Serine	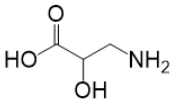 Isoserine*	
C_4	C_4	C_4
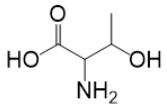 Threonine	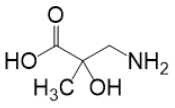 α-Methylisoserine**	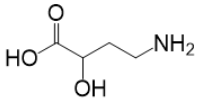 4-Amino-2-hydroxy-butanoic acid*
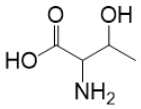 *allo*-Threonine	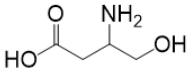 β-Homoserine*	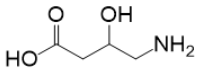 4-Amino-3-hydroxy-butanoic acid*
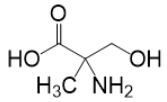 α-Methylserine*	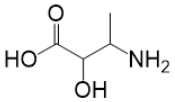 Isothreonine*	
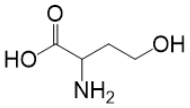 Homoserine*	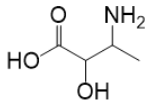 *allo*-Isothreonine*	
	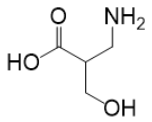 3-Amino-2-(hydroxy-methyl)propanoic acid*	

Fig. 1. All the structural isomers of C_3 and C_4 hydroxy amino acids investigated in this study.

* Hydroxy amino acids identified in the Murchison (CM2) meteorite by Koga and Naraoka (2017).

** Although a peak whose mass spectrum corresponding to the structure of α-methylisoserine was detected in the Murchison meteorite by Koga and Naraoka (2017), proper identification of the peak was not possible in that reporting due to the unavailability of the necessary analytical standard.

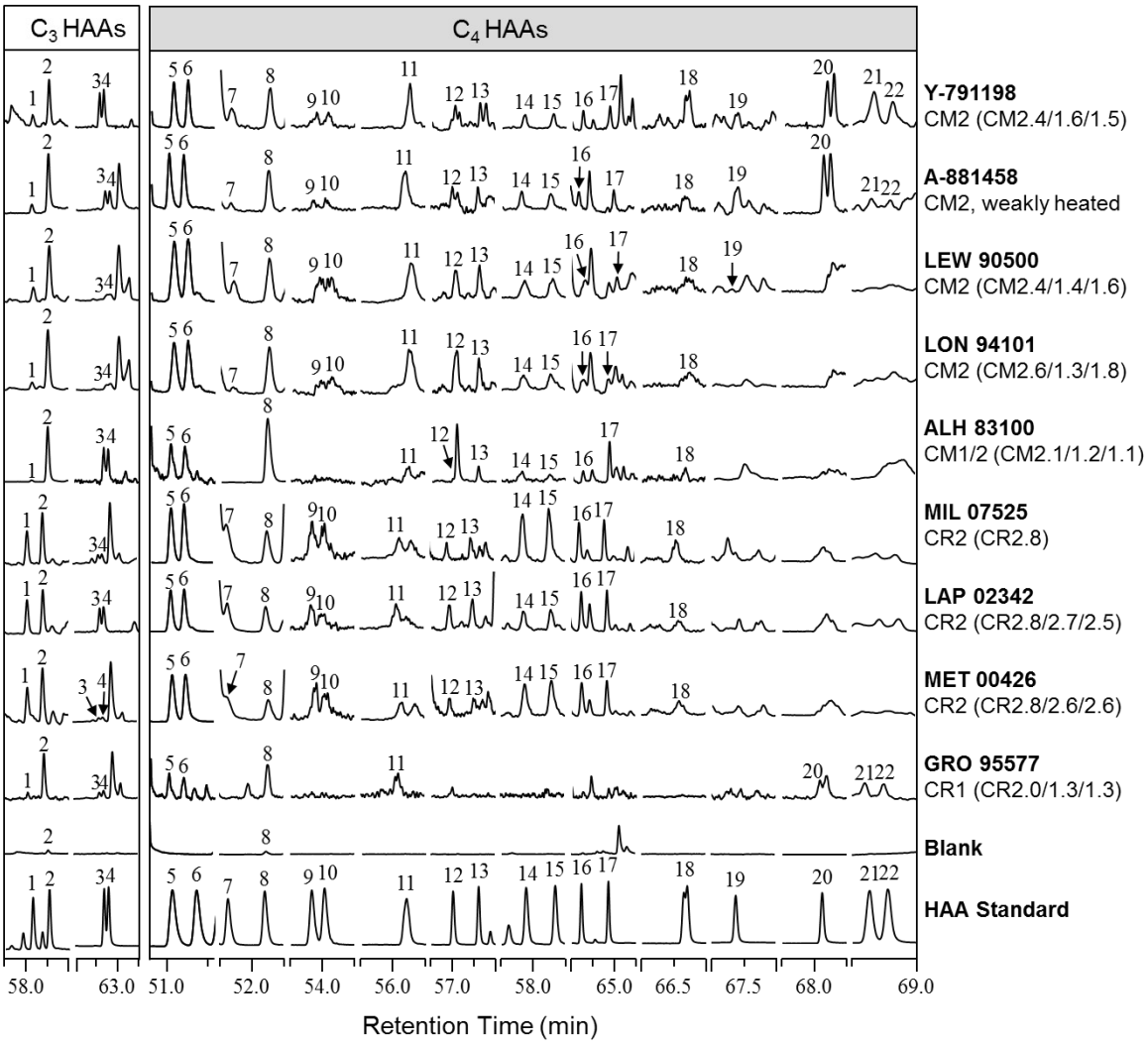

779 Fig. 2. The selected regions of the GC-MS extracted ion chromatograms of the C_3
780 and C_4 hydroxy amino acids in the HW extracts of the CM and CR chondrites studied
781 here. Peak identifications are as follows: 57.5–59.0 min for 1) D-serine and 2) L-
782 serine; 62.0–63.5 min for 3) D-isoserine and 4) L-isoserine; 50.6–51.6 min for 5) L-α-
783 methylserine and 6) D-α-methylserine; 51.5–52.5 min for 7) D-threonine and 8) L-
784 threonine; 53.5–54.5 min for 9) D- or L-isothreonine and 10) D- or L-isothreonine;
785 55.5–56.5 min for 11) DL-α-methylisoserine; 56.5–58.0 min for 12) D-*allo*-threonine
786 and 13) L-*allo*-threonine; 57.5–58.5 min for 14) D- or L-*allo*-isothreonine and 15) D-
787 or L-*allo*-isothreonine; 64.0–65.5 min for 16) D-homoserine and 17) L-homoserine;
788 66.0–67.0 min for 18) DL-β-homoserine; 67.0–68.0 min for 19) D-3-A-2-HMPA; 67.5–
789 68.5 min for 20) L-4-A-2-HBA; and 68.5–69.0 min for 21) D-4-A-3-HBA and 22) L-4-
790 A-3-HBA. The fragment ions used to generate each chromatogram shown here are
791 detailed in **Table S1**.

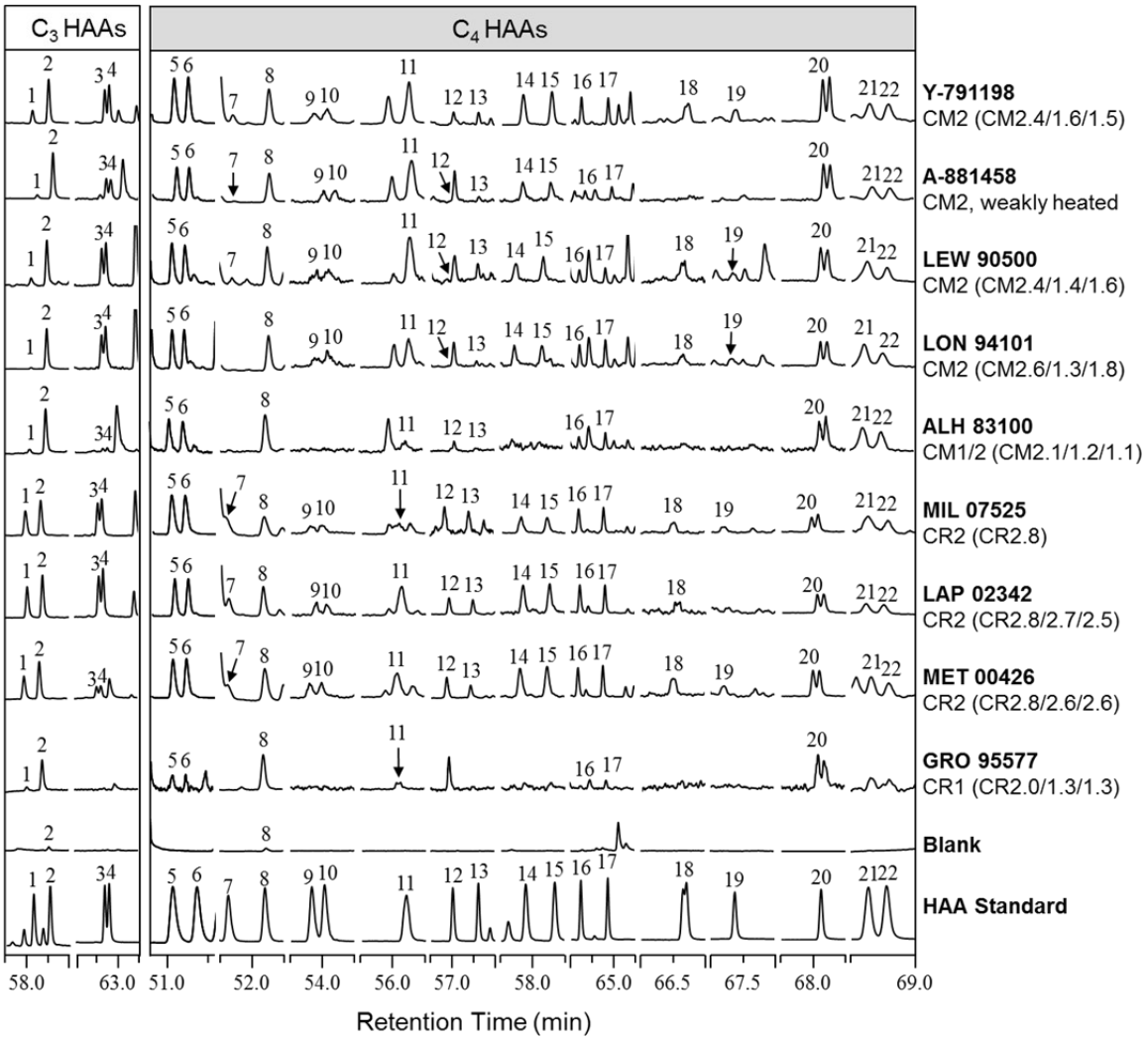

793 Fig. 3. The selected regions of the GC-MS extracted ion chromatograms of the C_3
794 and C_4 hydroxy amino acids in the 6 M HCl extracts of the CM and CR chondrites
795 studied here. Peak identifications are the same as in Fig. 2. The fragment ions used
796 to generate each chromatogram shown here are detailed in **Table S1**.

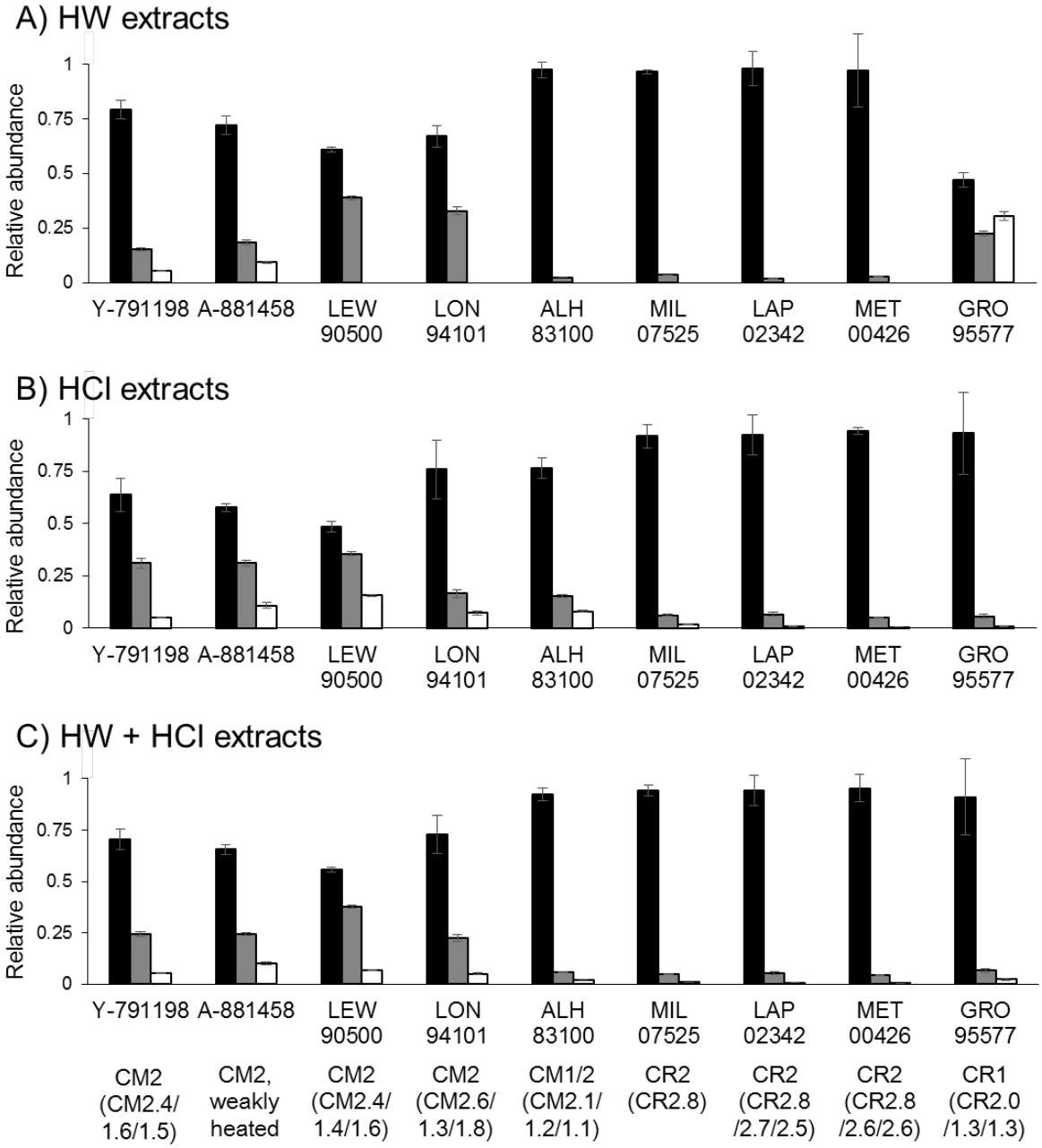

797 Fig. 4. The relative abundances of C_3 and C_4 hydroxy amino acids in CM and CR
798 carbonaceous chondrites for A) the HW extracts, B) the HCl extracts, and C) the
799 combined (HW + HCl) extracts. Relative abundances are displayed as functions of
800 amine position (α-, β-, γ-) relative to the total abundances of C_3 and C_4 hydroxy
801 amino acids. The relative abundances were calculated from the data in Tables 2 and
802 3, and the uncertainties were determined by appropriate propagation of the standard
803 errors. In all figure panes, black bars denote α-amines, grey bars denote β-amines,
804 and white bars denote γ-amines.

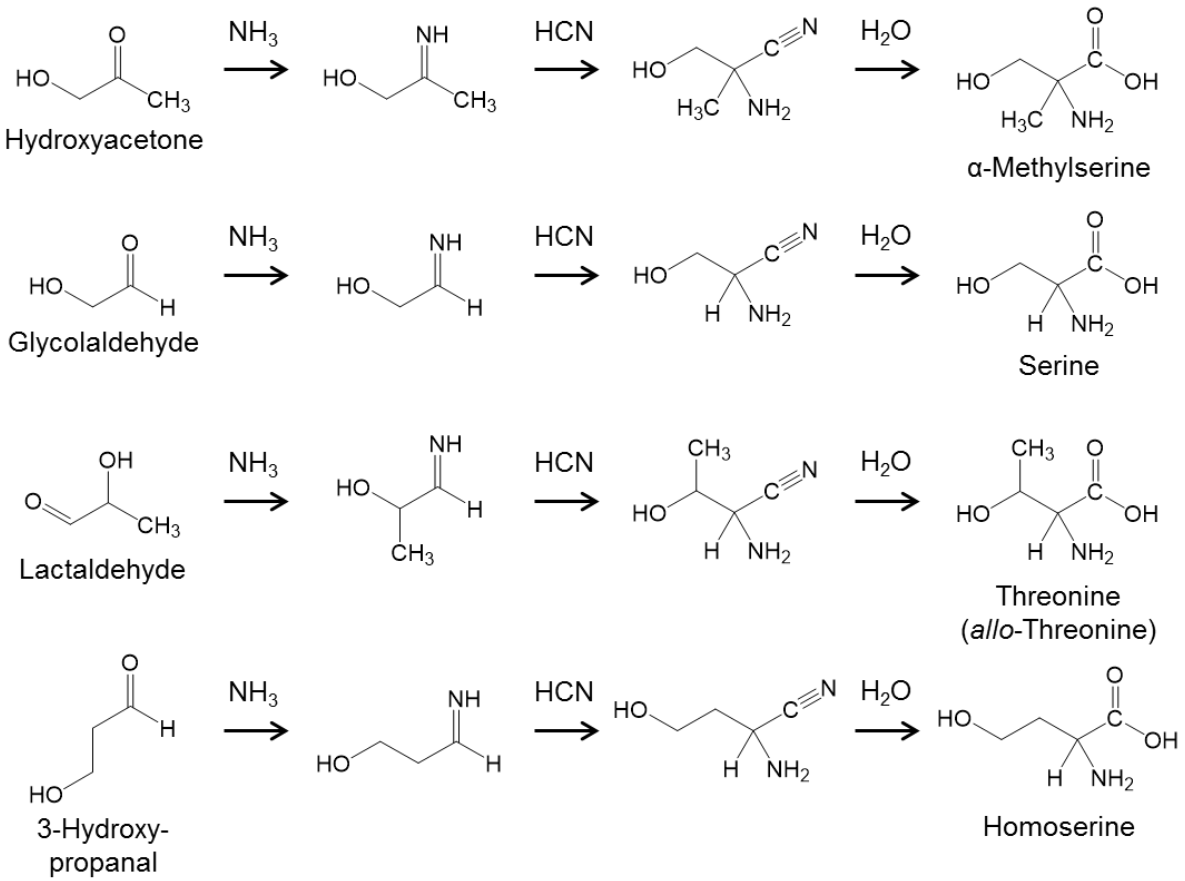

806 Fig. 5. Examples of the proposed synthetic pathways for the formation of select α-
807 hydroxy amino acids via the Strecker cyanohydrin reaction. It must be noted that α-
808 hydroxy amino acids could also be synthesized by an ammonia-involved formose-
809 like reaction as described by Koga and Naraoka (2017).

TABLES

Table 1. Meteorite samples analyzed in this study.

Meteorite[a]	Petrographic Type	Subtype (petrology)	Subtype (phyllosilicate fraction)[b]	Subtype (H in OH/H_2O)[c]	Mass extracted (mg)	Fragment (specific, parent)
Y-791198	CM2	2.4[d]	1.6	1.5	138.9	
A-881458	CM2, very weakly heated[e]	–	–	–	176.4	
LEW 90500	CM2	2.4[f]	1.4	1.6	364.4	89, 2
LON 94101	CM2	2.6[f]	1.3	1.8	274.0	101, 8
ALH 83100	CM1/2	2.1[f]	1.2	1.1	280.4	302, 279
MIL 07525	CR2[g]	2.8[h]	–	–	273.1	17, 0
LAP 02342	CR2	2.8[h]	2.7	2.5	298.1	64, 0
MET 00426	CR2	2.8[h]	2.6	2.6	327.3	78, 0
GRO 95577	CR1	2.0[h]	1.3	1.3	342.1	9, 0

[a] Abbreviations: Asuka, A-; Yamato, Y-; Lewis Cliffs, LEW; Lonewolf Nunataks, LON; Allan Hills, ALH; Miller Range, MIL; Meteorite Hills, MET; La Paz Icefield, LAP; Grosvenor Mountains, GRO.

[b] After Howard et al. (2015).

[c] After Alexander et al. (2013).

[d] After Rubin et al. (2007)

[e] After Nakamura (2005) and Kimura et al. (2011).

[f] Estimated using correlations between petrologic type and bulk H and N isotopes from Alexander et al. (2013).

[g] Although Antarctic Meteorite Newsletter, 34 and NASA Antarctic Meteorite Petrographic Description (https://curator.jsc.nasa.gov/antmet/samples/petdes.cfm?sample=MIL07525, accessed on 4/22/2021) classified MIL 07525 as a CR3, subsequent reporting (*e.g.,* Vollmer et al. 2020) has regarded MIL 07525 as a CR2 because of abundant secondary phases.

[h] After Harju et al. (2014).

Table 2. Summary of the average abundances (nmol/g) of the three- to four-carbon hydroxy amino acids identified in the HW and HCl extracts of CM carbonaceous chondrites measured by GC-MS[a].

Hydroxy amino acids	Y-791198		A-881458		LEW 90500		LON 94101		ALH 83100	
	CM2		CM2		CM2		CM2		CM1/2	
(Amine position)	Hot water	HCl	Hot water	HCl	Hot water	HCl	Hot water	HCl	Hot water	HCl
D-Serine (α)	4.2[b]	7 ± 2	0.29 ± 0.01	0.67 ± 0.03	0.088 ± 0.007	0.137 ± 0.005	0.12 ± 0.02	0.26 ± 0.05	0.16 ± 0.01	0.14 ± 0.01
L-Serine (α)	9.5[b]	18 ± 4	2.2 ± 0.2	1.60 ± 0.07	0.24 ± 0.03	0.69 ± 0.07	0.7 ± 0.1	2.1 ± 0.5	5.0 ± 0.2	1.05 ± 0.09
DL-Isoserine[e] (β)	1.40 ± 0.03	8.2 ± 0.4	0.53 ± 0.02	0.46 ± 0.03	0.44 ± 0.02	0.149 ± 0.006	0.369 ± 0.008	0.125 ± 0.009	0.133 ± 0.004	0.41 ± 0.01
L-α-Methylserine (α)	12 ± 1	7.8 ± 0.5	1.13 ± 0.07	0.366 ± 0.009	0.749 ± 0.009	0.133 ± 0.001	0.272 ± 0.003	0.20 ± 0.03	0.034 ± 0.002	0.126 ± 0.004
D-α-Methylserine (α)	13 ± 1	7.9 ± 0.5	1.2 ± 0.1	0.38 ± 0.01	0.76 ± 0.01	0.127 ± 0.002	0.261 ± 0.001	0.19 ± 0.02	0.0347 ± 0.0005	0.120 ± 0.006
D-Threonine (α)	0.40[d] ± 0.07	0.35[d] ± 0.05	0.033 ± 0.004	0.019 ± 0.007	0.061[d] ± 0.002	0.0140 ± 0.0002	0.013 ± 0.001	0.013 ± 0.001	n.d.	n.d.
L-Threonine (α)	0.6 ± 0.1	1.2 ± 0.2	0.22 ± 0.01	0.75 ± 0.04	0.106 ± 0.004	0.077 ± 0.002	0.124 ± 0.003	0.41 ± 0.05	1.66 ± 0.06	0.35 ± 0.01
D-*allo*-Threonine (α)	0.14[d] ± 0.02	0.22 ± 0.02	0.034[d] ± 0.003	0.017[d]	0.059[d] ± 0.003	0.012[d]	0.018[d]	0.017[d]	0.054[d]	0.013[d]
L-*allo*-Threonine (α)	0.19[d] ± 0.04	0.22 ± 0.02	0.036[d] ± 0.003	0.017 ± 0.003	0.050 ± 0.004	0.012 ± 0.001	0.018 ± 0.002	0.017[d] ± 0.001	0.054 ± 0.004	0.013 ± 0.001
D-Homoserine (α)	0.62[d] ± 0.07	0.99[d] ± 0.04	0.35 ± 0.02	0.063 ± 0.006	0.084[d]	0.079 ± 0.005	0.040[d] ± 0.002	0.067 ± 0.009	0.033 ± 0.001	0.0249 ± 0.0005
L-Homoserine (α)	0.61 ± 0.07	0.97 ± 0.04	0.37 ± 0.01	0.084[d] ± 0.001	0.084[d] ± 0.005	0.079 ± 0.003	0.038[d] ± 0.001	0.08 ± 0.01	0.105 ± 0.002	0.0293 ± 0.0008
DL-α-Methylisoserine[e] (β)	5.4 ± 0.2	14.6 ± 0.8	0.86 ± 0.07	1.91 ± 0.09	0.97 ± 0.02	0.85 ± 0.01	0.33 ± 0.02	0.57[d] ± 0.02	0.045 ± 0.006	0.060 ± 0.006
DL-Isothreonine[f] (β)	0.6 ± 0.1	1.8 ± 0.2	0.18 ± 0.03	0.119 ± 0.006	0.23 ± 0.01	0.087 ± 0.007	0.09 ± 0.02	0.08 ± 0.01	n.d.	n.d.
DL-allo-Isothreonine[f] (β)	0.50 ± 0.03	1.11 ± 0.04	0.095 ± 0.007	0.089 ± 0.006	0.122 ± 0.006	0.048 ± 0.001	0.086 ± 0.006	0.041 ± 0.005	0.019 ± 0.002	n.d.
DL-β-Homoserine[e] (β)	0.98 ± 0.04	0.72 ± 0.03	0.073 ± 0.007	n.d.	0.064 ± 0.002	0.079 ± 0.004	0.08 ± 0.01	0.074 ± 0.002	0.025 ± 0.002	n.d.
D-3-A-2-HMPA[g] (β)	1.0[d] ± 0.1	0.7 ± 0.1	0.131[d] ±0.008	0.11 ± 0.02	n.d.	0.027[d] ± 0.002	n.d.	0.034[d] ± 0.002	n.d.	n.d.
L-4-A-2-HBA[g] (γ)	0.78[d] ± 0.04	1.52 ± 0.08	0.28 ± 0.01	0.24 ± 0.04	n.d.	0.093 ± 0.003	n.d.	0.072 ± 0.008	n.d.	0.038 ± 0.001
D-4-A-3-HBA (γ)	0.352[d] ± 0.002	0.121 ± 0.005	0.056[d] ± 0.006	0.08[d] ± 0.01	n.d.	0.084[d] ± 0.001	n.d.	0.062[d] ± 0.003	n.d.	0.036[d] ± 0.002
L-4-A-3-HBA (γ)	0.23 ± 0.01	0.132 ± 0.007	0.042 ± 0.005	0.06 ± 0.01	n.d.	0.044 ± 0.002	n.d.	0.031 ± 0.002	n.d.	0.0243 ± 0.0008
Total (nmol/g)	52 ± 2[g]	74 ± 5	8.1 ± 0.3	7.0 ± 0.1[g]	4.12 ± 0.05[g]	2.8 ± 0.1[g]	2.5 ± 0.1[g]	4.5 ± 0.5[g]	7.4 ± 0.2[g]	2.43 ± 0.09[g]

Sum of HW & HCl (nmol/g)	126 ± 5[g]	15.2 ± 0.3[g]	6.94 ± 0.09[g]	7.0 ± 0.5[g]	9.8 ± 0.2[g]
HW / (HW + HCl)	41 %	54 %	59 %	36 %	75 %

n.d. = value not determined due to trace amino acid abundances.

[a] Sample extracts were analyzed by HFBA-isopropyl derivatization and GC-MS. The reported uncertainties (δx) are based on the standard deviation value (σx) of 2-3 separate measurements (n) with a standard error, $\delta x = \sigma x \cdot (n)^{-1/2}$.

[b] Minimum abundances are shown without an accompanying standard error because replicate measurements of this analyte were not made.

[c] The enantiomers were not resolved by the chromatographic separation applied in this study.

[d] The abundances and their associated uncertainties presented here are approximate due to quantitative interferences posed by coeluting species (*e.g.,* non-HAA species or D-α-methylserine coeluting with D-threonine) in the meteorite sample.

[e] The abundances were reported as the combined quantity estimates of both enantiomers because although the enantiomers were separated, the elution orders of the respective enantiomers were not determined due to a lack of enantiopure standard availability.

[f] Precise abundance estimates are not provided due to the lack of enantiopure standards. Instead, upper limit abundances were estimated.

[g] Total abundances were determined using individual HAA abundance estimates that were not accompanied by a standard error, which may cause the true uncertainties of the total abundance estimates to be larger than the total uncertainty estimates provided here.

Table 3. Summary of the average abundances (nmol/g) of the three- to four-carbon hydroxy amino acids identified in the HW and HCl extracts of CR carbonaceous chondrites measured by GC-MS[a].

	MIL 07525		LAP 02342		MET 00426		GRO 95577	
Hydroxy amino acids	CR2		CR2		CR2		CR1	
(Amine position)	Hot water	HCl	Hot water	HCl	Hot water	HCl	Hot water	HCl
D-Serine (α)	11[b]	25[b]	1.9 ± 0.2	51 ± 7	23 ± 8	38 ± 1	0.0166 ± 0.0005	1.3 ± 0.2
L-Serine (α)	12[b]	27[b]	2.1 ± 0.2	52 ± 7	23 ± 10	46 ± 1	0.13 ± 0.01	6 ± 1
DL-Isoserine[e] (β)	1.44 ± 0.09	5.5 ± 0.5	0.43 ± 0.03	1.2 ± 0.1	0.98 ± 0.07	3.1 ± 0.1	0.085 ± 0.005	0.075 ± 0.004
L-α-Methylserine (α)	60.9 ± 0.7	34 ± 4	20 ± 2	14 ± 2	24 ± 1	29.5 ± 0.2	0.0154 ± 0.0003	0.051 ± 0.004
D-α-Methylserine (α)	67.9 ± 0.6	38 ± 4	23 ± 2	14 ± 2	26 ± 2	33.6 ± 0.4	0.014 ± 0.001	0.051 ± 0.001
D-Threonine (α)	2.78[d] ± 0.04	1.4[d] ± 0.2	1.3[d] ± 0.1	1.1[d] ± 0.2	0.047[d] ± 0.02	1.6[d] ± 0.1	n.d.	n.d.
L-Threonine (α)	2.68 ± 0.05	1.8 ± 0.2	1.2 ± 0.1	1.4[d] ± 0.3	0.84 ± 0.06	3.73 ± 0.06	0.040 ± 0.006	1.3 ± 0.3
D-*allo*-Threonine (α)	1.81 ± 0.05	0.8 ± 0.1	2.1[d] ± 0.8	0.5 ± 0.1	0.7[d] ± 0.1	1.22 ± 0.04	n.d.	n.d.
L-*allo*-Threonine (α)	2.42[d] ± 0.09	0.7 ± 0.1	2.2[d] ± 0.8	0.45 ± 0.08	0.80[d] ± 0.03	1.32[d] ± 0.04	n.d.	n.d.
D-Homoserine (α)	1.33[d] ± 0.08	1.5[d] ± 0.1	0.54[d] ± 0.03	0.48[d] ± 0.03	1.46[d] ± 0.08	1.02 ± 0.04	0.0049[d] ± 0.0005	0.022[d] ± 0.002
L-Homoserine (α)	1.16 ± 0.08	1.5[d] ± 0.1	0.49 ± 0.02	0.45 ± 0.03	1.36 ± 0.09	0.98 ± 0.05	0.0042[d] ± 0.0003	0.0475[d] ± 0.0007
DL-α-Methylisoserine[e] (β)	2.8 ± 0.1	1.9[d] ± 0.2	0.33 ± 0.04	10 ± 2	1.3 ±0.1	4.0 ± 0.1	0.047 ± 0.003	0.61 ± 0.01
DL-Isothreonine[f] (β)	1.7 ± 0.1	2.1 ± 0.2	0.272 ± 0.002	0.54 ± 0.06	0.68 ± 0.03	2.42 ± 0.09	n.d.	n.d.
DL-allo-Isothreonine[f] (β)	0.87 ± 0.02	0.85 ± 0.08	0.084[d] ± 0.004	0.16 ± 0.01	0.306 ± 0.008	0.68 ± 0.01	n.d.	n.d.
DL-β-Homoserine[e] (β)	0.51 ± 0.04	0.55 ± 0.04	0.098 ± 0.003	0.119 ± 0.009	0.40 ± 0.03	0.259 ± 0.006	n.d.	n.d.
D-3-A-2-HMPA[g] (β)	n.d.	0.26[d] ± 0.02	n.d.	0.0102[d] ± 0.002	n.d.	0.082 ± 0.003	n.d.	n.d.
L-4-A-2-HBA[g] (γ)	n.d.	0.8 ± 0.1	n.d.	0.38 ± 0.01	n.d.	0.37 ± 0.02	0.041 ± 0.003	0.040 ± 0.003
D-4-A-3-HBA (γ)	n.d.	0.34[d] ± 0.03	n.d.	0.15[d] ± 0.01	n.d.	0.090[d] ± 0.003	0.017[d] ± 0.001	n.d.
L-4-A-3-HBA (γ)	n.d.	0.20 ± 0.03	n.d.	0.12 ± 0.01	n.d.	0.073 ± 0.004	0.013 ± 0.002	n.d.
Total (nmol/g)	171 ± 1[g]	144 ± 6[g]	56 ± 3	148 ± 10	110 ± 10	168 ± 2	0.42 ± 0.01	10 ± 1
Sum of HW & HCl (nmol/g)	315 ± 6[g]		200 ± 10		270 ± 10		10 ± 1	
HW / (HW + HCl)	54 %		27 %		39 %		4 %	

n.d. = value not determined due to trace amino acid abundances.

[a] Sample extracts were analyzed by HFBA-isopropyl derivatization and GC-MS. The reported uncertainties (δx) are based on the standard deviation value (σ) of 2-3 separate measurements (n) with a standard error, $\delta x = \sigma x \cdot (n)^{-1/2}$.

[b] Minimum abundances are shown without an accompanying standard error because replicate measurements of this analyte were not made.

[c] The enantiomers were not resolved by the chromatographic separation applied in this study.

[d] The abundances and their associated uncertainties presented here are approximate due to quantitative interferences posed by coeluting species (*e.g.,* non-HAA species or D-α-methylserine coeluting with D-threonine) in the meteorite sample.

[e] The abundances were reported as the combined quantity estimates of both enantiomers because although the enantiomers were separated, the elution orders of the respective enantiomers were not determined due to a lack of enantiopure standard availability.

[f] Precise abundance estimates are not provided due to the lack of enantiopure standards. Instead, upper limit abundances were estimated.

[g] Total abundances were determined using individual HAA abundance estimates that were not accompanied by a standard error, which may cause the true uncertainties of the total abundance estimates to be larger than the total uncertainty estimates provided here.

Table 4. Summary of the combined abundances (nmol/g) of the three- to four-carbon hydroxy amino acids in the two extracts (HW + HCl extracts) of CM and CR carbonaceous chondrites measured by GC-MS[a].

Hydroxy amino acids (Amine position)	Y-791198 CM2 HW + HCl	A-881458 CM2 HW + HCl	LEW 90500 CM2 HW + HCl	LON 94101 CM2 HW + HCl	ALH 83100 CM1/2 HW + HCl	MIL 07525 CR2 HW + HCl	LAP 02342 CR2 HW + HCl	MET 00426 CR2 HW + HCl	GRO 95577 CR1 HW + HCl
D-Serine (α)	11 ± 2[b]	0.97 ± 0.04	0.225 ± 0.009	0.37 ± 0.05	0.30 ± 0.02	36[c]	53 ± 7	62 ± 8	1.3 ± 0.2
L-Serine (α)	28 ± 4[b]	3.8 ± 0.3	0.94 ± 0.07	2.8 ± 0.5	6.1 ± 0.2	39[c]	54 ± 7	69 ± 10	6 ± 1
DL-Isoserine[e] (β)	9.6 ± 0.4	0.99 ± 0.03	0.59 ± 0.02	0.49 ± 0.01	0.54 ± 0.01	6.9 ± 0.5	1.6 ± 0.1	4.1 ± 0.1	0.160 ± 0.006
L-α-Methylserine (α)	20 ± 1	1.50 ± 0.07	0.882 ± 0.009	0.47 ± 0.03	0.160 ± 0.004	95 ± 4	33 ± 3	53 ± 1	0.067 ± 0.004
D-α-Methylserine (α)	21 ± 1	1.5 ± 0.1	0.89 ± 0.01	0.45 ± 0.02	0.155 ± 0.006	106 ± 4	38 ± 3	60 ± 2	0.066 ± 0.002
D-Threonine (α)	0.75[e] ± 0.09	0.052 ± 0.008	0.075[e] ± 0.002	0.026 ± 0.002	n.d.	4.2[e] ± 0.2	2.3[e] ± 0.2	2.1[e] ± 0.1	n.d.
L-Threonine (α)	1.8 ± 0.2	0.97 ± 0.04	0.183 ± 0.004	0.54 ± 0.05	2.01 ± 0.06	4.5 ± 0.2	2.6[e] ± 0.3	4.58 ± 0.08	1.3 ± 0.3
D-*allo*-Threonine (α)	0.36[e] ± 0.02	0.052[e] ± 0.005	0.071[e] ± 0.003	0.036[e] ± 0.002	0.068[e] ± 0.004	2.6 ± 0.1	2.6[e] ± 0.8	1.9[e] ± 0.1	n.d.
L-*allo*-Threonine (α)	0.41[e] ± 0.04	0.053[e] ± 0.005	0.062 ± 0.004	0.036[e] ± 0.002	0.068 ± 0.004	3.2[e] ± 0.1	2.6[e] ± 0.8	2.12[e] ± 0.05	n.d.
D-Homoserine (α)	1.61[e] ± 0.08	0.41 ± 0.02	0.163[e] ± 0.007	0.107[e] ± 0.009	0.058 ± 0.001	2.8[e] ± 0.2	1.02[e] ± 0.04	2.48[e] ± 0.09	0.027[e] ± 0.002
L-Homoserine (α)	1.58 ± 0.08	0.45[e] ± 0.01	0.163[e] ± 0.006	0.12[e] ± 0.01	0.134 ± 0.002	2.6[e] ± 0.1	0.94 ± 0.04	2.3 ± 0.1	0.0518[e] ± 0.0008
DL-α-Methylisoserine[e] (β)	20.0 ± 0.8	2.8 ± 0.1	1.82 ± 0.03	0.90[e] ± 0.03	0.105 ± 0.008	4.7[e] ± 0.2	10 ± 2	5.3 ± 0.2	0.66 ± 0.01
DL-Isothreonine[f] (β)	2.5 ± 0.2	0.30 ± 0.03	0.32 ± 0.01	0.17 ± 0.02	n.d.	3.7 ± 0.3	0.81 ± 0.06	3.1 ± 0.1	n.d.
DL-allo-Isothreonine[f] (β)	1.61 ± 0.05	0.184 ± 0.009	0.170 ± 0.006	0.127 ± 0.007	0.019 ± 0.002	1.72 ± 0.09	0.24[e] ± 0.01	0.99 ± 0.02	n.d.
DL-β-Homoserine[e] (β)	1.69 ± 0.05	0.073 ± 0.007	0.143 ± 0.004	0.16 ± 0.01	0.025 ± 0.002	1.06 ± 0.05	0.217 ± 0.009	0.66 ± 0.03	n.d.
D-3-A-2-HMPA[g] (β)	1.7[e] ± 0.2	0.24[e] ± 0.02	0.027[e] ± 0.002	0.034[e] ± 0.002	n.d.	0.26[e] ± 0.02	0.102[e] ± 0.002	0.082 ± 0.003	n.d.
L-4-A-2-HBA[g] (γ)	2.30[e] ± 0.09	0.52 ± 0.04	0.093 ± 0.003	0.072 ± 0.008	0.038 ± 0.001	0.81 ± 0.07	0.38 ± 0.01	0.37 ± 0.02	0.081 ± 0.005
D-4-A-3-HBA (γ)	0.474[e] ± 0.005	0.13[e] ± 0.01	0.084[e] ± 0.001	0.062[e] ± 0.003	0.036[e] ± 0.002	0.34[e] ± 0.03	0.15[e] ± 0.01	0.090[e] ± 0.003	0.017[e] ± 0.001
L-4-A-3-HBA (γ)	0.37 ± 0.01	0.10 ± 0.01	0.044 ± 0.002	0.031 ± 0.002	0.0243 ± 0.0008	0.20 ± 0.03	0.12 ± 0.01	0.073 ± 0.004	0.013 ± 0.002
Total of α-HAAs	85 ± 5[h]	9.9 ± 0.3[h]	3.65 ± 0.08[h]	4.9 ± 0.5[h]	9.0 ± 0.2[h]	296 ± 6[h]	190 ± 10	260 ± 10	9 ± 1
Total of β-HAAs	37.1 ± 0.9	4.6 ± 0.1	3.07 ± 0.04	1.89 ± 0.04	0.69 ± 0.02	18.4 ± 0.6	13 ± 2	14.2 ± 0.3	0.82 ± 0.01
Total of γ-HAAs	3.14 ± 0.09	0.75 ± 0.04	0.220 ± 0.004	0.164 ± 0.009	0.098 ± 0.002	1.3 ± 0.1	0.65 ± 0.02	0.53 ± 0.02	0.112 ± 0.005
Sum of HW & HCl (nmol/g)	126 ± 5[h]	15.2 ± 0.3[h]	6.94 ± 0.09[h]	7.0 ± 0.5[h]	9.8 ± 0.2[h]	315 ± 6[h]	200 ± 10	270 ± 10	10 ± 1

n.d. = value not determined due to trace amino acid abundances.

[a] The combined abundances in the HW and HCl extracts were summed from Table 2 and 3, and the uncertainties ($\delta x_{combined}$) were propagated through the relevant equations with $\delta x_{combined} = (\delta x_{HW}^2 + \delta x_{HCl}^2)^{1/2}$.

[b] Combined abundances were determined using individual HAA abundance estimates that were not accompanied by a standard error, which may cause the true uncertainties of the total abundance estimates to be larger than the total uncertainty estimates provided here.

[c] Minimum abundances are shown without an accompanying standard error because replicate measurements of this analyte were not made.

[d] The enantiomers were not resolved by the chromatographic separation applied in this study.

[e] The abundances and their associated uncertainties presented here are approximate due to quantitative interferences posed by coeluting species (*e.g.,* non-HAA species or D-α-methylserine coeluting with D-threonine) in the meteorite sample.

[f] The abundances were reported as the combined quantity estimates of both enantiomers because although the enantiomers were separated, the elution orders of the respective enantiomers were not determined due to a lack of enantiopure standard availability.

[g] Precise abundance estimates are not provided due to the lack of enantiopure standards. Instead, upper limit abundances were estimated.

[h] Total abundances were determined using individual HAA abundance estimates that were not accompanied by a standard error, which may cause the true uncertainties of the total abundance estimates to be larger than the total uncertainty estimates provided here.

Table 5. Summary of D/L ratios and L-enantiomeric excesses (L_{ee}) measured for several α-hydroxy amino acids in the HW and HCl extracts of CM and CR chondrites[a].

	Y-791198 CM2		A-881458 CM2		LEW 90500 CM2		LON 94101 CM2		ALH 83100 CM1/2	
	Hot water	HCl	Hot water	HCl	Hot water	HCl	Hot water	HCl	Hot water	HCl
	D/L ratio (%Lee)	D/L ratio (%Lee)	D/L ratio (%Lee)	D/L ratio (%Lee)	D/L ratio (%Lee)	D/L ratio (%Lee)	D/L ratio (%Lee)	D/L ratio (%Lee)	D/L ratio (%Lee)	D/L ratio (%Lee)
Serine (α)	[b]	0.35 ± 0.12 (47.9 ± 10.0)	0.13 ± 0.02 (76.8 ± 1.7)	0.42 ± 0.03 (40.8 ± 2.1)	0.36 ± 0.05 (47.0 ± 4.2)	0.20 ± 0.02 (66.9 ± 2.0)	0.17 ± 0.04 (70.3 ± 4.1)	0.12 ± 0.04 (78.4 ± 4.0)	0.031 ± 0.002 (93.9 ± 0.3)	0.13 ± 0.02 (76.6 ± 1.9)
α-Methylserine (α)	1.06 ± 0.15 (-2.7 ± 7.2)	1.02 ± 0.08 (-0.9 ± 4.2)	1.03 ± 0.11 (-1.5 ± 5.3)	1.03 ± 0.04 (-1.2 ± 2.0)	1.02 ± 0.02 (-1.0 ± 0.9)	0.95 ± 0.02 (2.4 ± 0.8)	0.96 ± 0.01 (1.9 ± 0.6)	0.97 ± 0.18 (1.4 ± 9.1)	1.02 ± 0.05 (-1.0 ± 2.4)	0.95 ± 0.05 (2.4 ± 2.7)
Threonine (α)	[d]	[d]	0.15 ± 0.02 (74.2 ± 2.2)	0.02 ± 0.01 (95.2 ± 1.3)	[d]	0.18 ± 0.01 (69.2 ± 0.7)	0.11 ± 0.01 (80.7 ± 1.3)	0.032 ± 0.005 (93.8 ± 0.7)	[c]	[c]
allo-Threonine (α)	[d]	0.99 ± 0.12 (0.3 ± 6.2)	[d]	[d]	[d]	[d]	[d]	[b]	[d]	[d]
Homoserine (α)	[d]	[d]	0.96 ± .06 (2.2 ± 3.3)	[d]	[d]	1.00 ± 0.07 (0.1 ± 3.5)	[d]	0.86 ± 0.17 (7.6 ± 9.2)	0.32 ± 0.01 (51.7 ± 1.2)	0.85 ± 0.03 (8.0 ± 1.6)

	MIL 07525 CR2		LAP 02342 CR2		MET 00426 CR2		GRO 95577 CR1	
	Hot water	HCl	Hot water	HCl	Hot water	HCl	Hot water	HCl
	D/L ratio (%Lee)	D/L ratio (%Lee)	D/L ratio (%Lee)	D/L ratio (%Lee)	D/L ratio (%Lee)	D/L ratio (%Lee)	D/L ratio (%Lee)	D/L ratio (%Lee)
Serine (α)	[b]	[b]	0.92 ± 0.12 (4.2 ± 6.2)	0.99 ± 0.19 (0.5 ± 9.5)	[b]	0.84 ± 0.04 (8.6 ± 1.9)	0.13 ± 0.01 (76.6 ± 1.4)	0.22 ± 0.05 (64.2 ± 5.3)
α-Methylserine (α)	1.11 ± 0.02 (-5.4 ± 0.8)	1.12 ± 0.18 (-5.5 ± 8.5)	1.18 ± 0.16 (-8.1 ± 7.3)	1.05 ± 0.23 (-2.6 ± 11.3)	1.10 ± 0.09 (-4.9 ± 4.3)	1.14 ± 0.02 (-6.6 ± 0.8)	0.94 ± 0.09 (3.3 ± 4.8)	1.00 ± 0.08 (0.0 ± 3.9)
Threonine (α)	[d]	[d]	[d]	[d]	[d]	[d]	[c]	[c]
allo-Threonine (α)	[d]	1.07 ± 0.22 (-3.2 ± 10.5)	[d]	[d]	[d]	[d]	n.d.	n.d.
Homoserine (α)	[d]	[d]	[d]	[d]	[d]	[d]	[d]	[d]

n.d. = not determined.

[a] The standard errors (δx) for D/L ratios and the L-enantiomeric excesses (L_{ee}) are based on the values and errors from Table 2 and Table 3 propagated through the relevant equations with L_{ee} = [(L-D)/(L+D)] · 100.

[b] The L-enantiomeric excesses were not reported because replicate measurements of this analyte were not made.

[c] The L-enantiomeric excesses could not be calculated because the concentration of the D-enantiomer was below the detection limit.

[d] L-enantiomeric excesses were not reported due to coelution with other chromatographic peaks.

877 Table S1. Summary of the fragment ions (*m/z*) used for quantification of each HAA in the CM and CR chondrites.

	Y-791198		A-881458		LEW 90500		LON 94101		ALH 83100		MIL 07525		LAP 02342		MET 00426		GRO 95577	
	CM2		CM2		CM2		CM2		CM1/2		CR2		CR2		CR2		CR1	
Hydroxy amino acids (Peak # in Fig. 2, 3)	HW	HCl	HW	HCl	HW	HCl	HW	HCl	HW	HCl	HW	HCl	HW	HCl	HW	HCl	HW	HCl
D-Serine (#1)	239	239	239	239	239	239	239	239	239	239	239	239	239	239	239	239	239	239
L-Serine (#2)	239	239	284	239	239	239	239	239	239	239	239	239	239	239	239	239	239	239
DL-Isoserine (#3 & 4)	452	239	239	239	239	452	239	452	452	239	239	239	452	452	239	452	239	239
L-α-Methylserine (#5)	252	252	252	252	252	252	252	252	252	252	252	252	252	252	252	252	252	252
D-α-Methylserine (#6)	252	252	252	252	252	252	252	252	252	252	252	252	252	252	252	252	252	252
D-Threonine (#7)	253	253	253	253	253	253	253	253	n.d.	n.d.	253	253	253	253	253	253	n.d.	n.d.
L-Threonine (#8)	253	253	253	253	253	253	253	253	253	253	253	253	253	253	253	253	253	253
Isothreonine (#9)	466	466	466	466	466	466	466	466	n.d.	n.d.	466	466	466	466	466	466	n.d.	n.d.
Isothreonine (#10)	466	466	466	466	466	466	466	466	n.d.	n.d.	466	466	466	466	466	466	n.d.	n.d.
DL-α-Methylisoserine (#11)	466	252	466	252	252	466	252	466	252	252	466	466	466	466	466	466	252	252
D-*allo*-Threonine (#12)	253	253	253	253	253	253	253	253	253	253	466	298	238	253	466	252	n.d.	n.d.
L-*allo*-Threonine (#13)	253	253	253	253	253	253	253	253	253	253	466	298	238	253	466	252	n.d.	n.d.
allo-Isothreonine (#14)	272	466	272	272	272	272	272	272	272	n.d.	272	272	272	272	272	272	n.d.	n.d.
allo-Isothreonine (#15)	272	466	272	272	272	272	272	272	272	n.d.	272	272	272	272	272	272	n.d.	n.d.
D-Homoserine (#16)	252	252	298	252	252	252	252	252	252	252	252	252	252	252	252	252	252	252
L-Homoserine (#17)	252	252	298	252	252	252	252	252	252	252	252	252	252	252	252	252	252	252
DL-β-Homoserine (#18)	494	494	494	n.d.	494	494	494	494	494	n.d.	494	494	494	494	494	494	n.d.	n.d.
D-3-A-2-HMPA (#19)	280	280	280	280	n.d.	280	n.d.	280	n.d.	n.d.	n.d.	280	n.d.	280	n.d.	280	n.d.	n.d.
L-4-A-2-HBA (#20)	466	466	466	466	n.d.	466	n.d.	466	n.d.	466	n.d.	466	n.d.	466	n.d.	466	466	466
D-4-A-3-HBA (#21)	252	252	280	252	n.d.	252	n.d.	252	n.d.	252	n.d.	280	n.d.	252	n.d.	280	252	n.d.
L-4-A-3-HBA (#22)	252	252	280	252	n.d.	252	n.d.	252	n.d.	252	n.d.	280	n.d.	252	n.d.	280	252	n.d.

878 n.d. = value not determined due to trace amino acid abundances.